

Enhancing the efficiency of evaporative cooling pads for livestock barns and greenhouses by moisture adsorption

M. Samer^{1*}, E. Abdelsalam², Y. B. Abd Elhay¹

(1. Department of Agricultural Engineering, Faculty of Agriculture, Cairo University, Giza 12613, Egypt;

2. National Institute of Laser Enhanced Sciences (NILES), Cairo University, Giza 12613, Egypt.)

Abstract: High levels of relative humidity negatively affect the efficiency of the evaporative cooling pads installed in livestock barns and greenhouses. Consequently, the productivity decreases causing economic losses. Therefore, this project aims at prototyping innovative dehumidifying/desiccant segments to be installed on the conventional cooling pads enabling them to provide suitable microclimate conditions, especially temperature and relative humidity, for animals and plants. The hypothesis is that desiccant segments adsorb air moisture before introducing the air into the pads; consequently, the treated air is then able to absorb more moisture from the cooling pads, i.e. the cooling pads evaporate more water in the treated air, where water evaporation requires heat energy which is absorbed from the treated air which results in decreasing the treated air temperature. Theoretical and experimental investigations were conducted, where 211 laboratory experiments were performed for testing this hypothesis. The theoretical investigations (calculations and designs) were conducted using the results of the lab experiments. This study presents a methodology for testing desiccant materials and assessing their suitability as filling for the desiccant segments. The water adsorption capacity was 125, 158, 257, 132, 142 g H₂O/kg desiccant, and the water adsorption rate was 17, 22, 36, 18, 20 g H₂O/(kg desiccant h) for ARTSorbTM, PROSorbTM, Silica Gel, Silica Gel Macro-porous, and the mixture of all 4 desiccants, respectively. Model calculations showed that the required amount of desiccant per unit area of pads is 70 kg/m². The thickness of the desiccant segments is 10 cm, with a total pressure drop of 0.6 kPa under the toughest conditions of air velocity of 2.5 m/s and 2 mm bead size. The desiccant segments require 0.18 kW extra energy per m² of pads to overcome the extra pressure drop, i.e. 63.5 kWh/m² and month which is the energy required by the extractor fans and costs 12.7 € / m² month approximately. The results show potential for developing a desiccant system to improving the efficiency of cooling pads for livestock barns and greenhouses.

Keywords: cooling pads, livestock housing, heat stress, indoor air quality, greenhouses

Citation: Samer M., E. Abdelsalam, and Y. B. Abd Elhay. 2016. Enhancing the efficiency of evaporative cooling pads for livestock barns and greenhouses by moisture adsorption. *Agric Eng Int: CIGR Journal*, 17(4):36-63.

1 Introduction

According to the Intergovernmental Panel on Climate Change (IPCC, 2007), changes in the climate are already causing setbacks to economic and social development in several countries with temperature increases of less than 1 °C. Unabated climate change would increase the risks and costs substantially. There may be risks associated with rapid and/or abrupt changes in the climate and the climate system as a result of human interference. These include changes in weather

variability, a high likelihood that warming will lead to an increased risk of many extreme events, including droughts and heat waves. Therefore, climate change adapted production systems should be developed in order to face the warming. Samer (2011a) stated that livestock production systems are dramatically affected by the increasing temperatures. Consequently, the production decreases and possible death occurs. One key solution is to implement cooling technologies, especially evaporative cooling systems which are suitable for livestock production and housing (Samer 2008a, 2011b, 2013a; Samer et al., 2008, 2012a). However, those cooling technologies are deficient when the outdoor air relative humidity exceeds 65% (Hatem, 1993).

Received date: 2015-07-31

Accepted date: 2015-09-28

*Corresponding author: M. Samer, Department of Agricultural Engineering, Faculty of Agriculture, Cairo University, 12613 Giza, Egypt. Email: msamer@agr.cu.edu.eg

Hence, they should be developed to enhance efficiency and applicability under tough conditions.

Wiersma and Short (1983) elucidated that animal confinement buildings are designed for cold weather conditions, but they have limited control of the environment during occasional hot spells in the summer. Severe summers result in significant death loss, if no relief is available. Therefore, evaporative cooling-pad systems (pads and extractor fans) were developed to be installed in closed buildings with forced ventilation. Furthermore, they discussed the theory of evaporative cooling. When non-saturated air comes in contact with free moisture, there is a transfer of mass and heat. Mass transfer occurs due to the vapour pressure difference, while this transfer involves a change of state from liquid to vapour, requiring latent heat of vaporization (2257.2 J/g) which comes from both the non-saturated air and the water, resulting in a drop in temperature of both. Koca et al. (1991) developed a procedure for testing evaporative cooling pads in order to relate efficiency, face air velocity, and static pressure drop across the pads. They added that four main characteristics can be used to rate a pad: cost, life, pressure drop, and efficiency. The cost of a pad is a function of the business market and pad design. The life of a pad is a function of pad design, water quality, air quality, and overall system design. Pressure drop and efficiency are affected by the pad design, pad thickness, air velocity, water flow rate, and age of the pad. Pressure drop versus air velocity is important for selecting a fan and pad area for a particular application. Efficiency is the most important physical performance factor. The more efficient a pad at a given air velocity, the more cooling it will provide.

Pads are normally run continuously along the side or end of the building opposite the exhaust fans. The pad height is generally between 0.5 m and 2.5 m when mounted vertically in order to achieve uniform water flow. The pads must expose the maximum amount of wetted surface area to the passing air for an adequate length of air water contact time to achieve near saturation.

Cooling pads should have a minimum amount of resistance to air flow. The pads must also be resistant to decay and retain their original shape and fibre orientation. Optimum aspen pads should approximate a density of 32 kg/m³ and a distribution of 4 kg/m², with higher density at the top to improve horizontal distribution at that level. The excelsior strands should have predominantly horizontal alignment. However, density of corrugated cellulose pad is 96.2 kg/m³. With density established, pad thickness can then be adjusted to the desired saturation efficiency or, preferably, maximum cooling per unit energy consumed. The recommended air face velocities through vertical pads are 0.75 m/s for aspen fibre (50-100 mm), 1.25 m/s for 100 mm-thick corrugated cellulose, and 1.75 m/s for 150 mm-thick corrugated cellulose. The recommended water flow rate per lineal length of pad for vertically mounted cooling pad materials are 5, 6, 10 L min⁻¹ m⁻¹ for aspen fibre (50-100 mm), 100 mm-thick, and 150 mm-thick corrugated cellulose, respectively. Where, the water application/recirculation rates are 2.4 L min⁻¹ m⁻² and 6 L min⁻¹ m⁻² of pad area for aspen and cellulose pads, respectively. In addition, 8 L/h bleed-off and 20-40 L/m² sump capacity should be considered (Dagtekin et al., 2009a; Liao et al., 1998; Koca et al., 1991; Wiersma and Short, 1983).

Panagakakis and Axaopoulos (2006) carried out simulation comparison between evaporative pads and fogging on air temperatures inside a growing swine building, and reduction of growing swine apparent heat stress. They proved that both cooling methods are significantly better compared to no cooling. Among all, evaporative pad was the most effective because it resulted in smaller daily inside dry-bulb temperature variation, maximum reduction of apparent heat stress intensity, and lower total water consumption. Bull et al. (1997) reported that the cooling pads are preferred over the drip coolers and the snout coolers by mature gilts. The cooling pads have significant effects on the physiological variables such as respiration rate and rectal temperature

which decrease when using the cooling pads, whereas the drip cooler and snout cooler have no effect on these variables. Johnson et al. (2000) mentioned that heat stress associated with elevated temperatures and relative humidity reduces the production levels of different swine facilities. Traditional cooling methods including evaporative pad cooling are used to lower temperature, but are not as effective in lowering relative humidity. They added, desiccant systems could be used to effectively eliminate stress conditions in a swine facility or modified to enhance current cooling methods.

Wang et al. (2008) stated that the average air temperature inside poultry houses could be lowered below 30 °C to 28 °C by using the evaporative pad cooling system for over 65% to 70% of the days when facing hot conditions. However, Dagtekin et al. (2009a) mentioned that a cooling efficiency of 69.35%, and a 5.19 °C decrease of the outside air temperature after passing through the pads, and a 1.52 °C increase in air temperature at the exit point, i.e. at the end of the barn, can be reached. Choi et al. (1998) stated that cooling pads decreased the house inside temperature to 5.4 °C in inlet site, 5.0 °C in middle site, 2.8 °C in outlet, but cooling effects of fogging system was very low. Relative humidity increased to 16.4% using cooling pads system with ventilation capacity of 0.195 cm³ per bird and air velocity lower than 1.5 m/s. Dagtekin et al. (2009a,b) mentioned that the most common ventilation system for barns is with ventilators. During hot summer periods, a fan ventilation system alone was not capable of cooling the interior space of the barn. They added that temperatures in Mediterranean regions frequently exceed 30 °C for long periods during summers. Pad evaporative cooling systems may provide a solution for controlling the high temperatures that can negatively affect poultry houses. Chicken meat and egg production shows enormous potential for growth. However, high temperatures in summer pose serious difficulties for these types of production. Evaporative cooling pads, 15 cm-thick cellulose-based pads, were widely used for providing cool

and moist air for animals during the summer season. Furthermore, they were used to minimize rises in temperature and are commonly used in poultry houses. However, this completely differs in naturally ventilated poultry houses (von Bobrutski, 2011). Bottcher et al. (1992) stated that the evaporative cooling pads system provided greater reduction in temperature at bird level than plastic ventilation ducts and pressure-controlled slot inlets.

Bucklin et al. (2009) stated that when relative humidity approaches high levels, the effectiveness of evaporative cooling is greatly reduced. Hence, providing comfortable environmental conditions for cows housed in areas with hot, humid climates is difficult using only evaporative cooling and ventilation. The optimal temperatures, i.e. thermoneutral zone, of several cow breeds, e.g. Holstein Friesian, are between 16 °C and 18 °C, and the upper critical temperature is 25 °C and the acceptable relative humidity ranges between 40% and 65% (Hall et al., 1997; Armstrong, 1994; Schmidt et al., 1988). According to Gebremedhin et al. (2010) and Gebremedhin et al. (2008), skin temperature is the primary driving force for sweating/evaporative cooling. The skin temperature threshold for heat stress is 35 °C. The maximum sweating rate of dairy cows is 660 g/m² h. Sweating rates are higher in hot and dry conditions because of the higher moisture gradient between skin surface and ambient air than that in hot and humid conditions. Jiang et al. (2005) mentioned that the skin temperature increased with increasing relative humidity, and evaporative heat loss increased with increasing ambient air temperature, wind speed, solar load, and hair density, but decreased with increasing relative humidity and hair coat thickness.

Huhnke et al. (2004) reported that extreme temperature and humidity can be harmful or even fatal to livestock if proper precautions are not taken. In other words, the combination of high humidity and high ambient temperatures can induce stress levels in animals that can be harmful, or even fatal, without proper

management. The evaporative cooling has the potential to eliminate severe conditions and is an effective method of reducing elevated environmental conditions. Mekonnen and Dodd (1993) studied the effectiveness of different microclimate modifiers for hot weather livestock housing in a model livestock building, where 100 mm thick cooling pads had higher saturation efficiency at air velocity 1.5 m/s and water flow rate of 3 L/min, with an acceptable level of relative humidity (under 60%). Subsequent to the high relative humidity levels (over 65%), the efficiency of the evaporative cooling decreases due to the high moisture content in the external air which result in decreasing the animal productivity (Samer, 2011a; Samer, 2004). Frazzi et al. (2002) mentioned that systems based on water evaporation are better suited to hot, dry climates than hot, humid ones. In addition, the style of the buildings and equipment can be important in the choice of cooling techniques. Hatem et al. (2004a,b) studied the effects of cowshed height and orientation on cooling efficiency and microclimatic conditions. Wang et al. (2008) stated that evaporative pad cooling systems are efficient in decreasing the inside air temperature of animal houses when encountering hot and dry conditions, but they are not suitable for hot and humid conditions. Mekonnen and Dodd (1993) reported that temperature reduction of 10 °C can be expected provided that the relative humidity of the supplied air does not exceed 60%.

Kiwan et al. (2012) investigated the effect of building equipment and operation on ventilation rate through dairy barns and concluded that the usually deployed equipment affect the ventilation rate. Kittas et al. (2003) studied the influence of different ventilation rates combined with shading on air temperature profiles along the greenhouse length and the influence of the outside air temperature and humidity on the performance of the cooling system. They added that the main drawback of greenhouse evaporative cooling systems based on cooling pads and extracting fans is the thermal gradient developed along the direction of the airflow.

High-temperature gradients of this type can markedly affect plant growth, and growers often combine cooling pads with shading. Gunhan et al. (2007) evaluated the suitability of pumice stones, volcanic tuff and greenhouse shading net as alternative pad materials to the widely used and commercial one called CELdek. They found that the volcanic tuff pads are good alternatives to the CELdek pads at 0.6 m/s air velocity. Al-Helal (2007) examined the influence of two ventilation rates on the environment of a shaded greenhouse equipped with fan-pad evaporative cooler in extreme arid conditions as well as the water consumption of the pads. The daytime average of water consumption with a ventilation rate of 0.5 and 1 ACM (air change per minute) were 8.4 L/m² and 14 L/m² of floor area, respectively.

Wind tunnels were widely implemented in agricultural research (Fiedler et al., 2011). Liao et al. (1998) performed wind tunnel experiments to obtain equations for heat and mass transfer coefficients for the evaporative process through various thicknesses of alternative pad media. They determined the cooling efficiency in a wind tunnel to relate efficiency, face velocity, and static pressure drop across pads. For a 15 cm pad, static pressure drops across nonwoven fabric perforated pad and cooling efficiencies varied from 48 Pa to 108 Pa and 81.2% to 81.9% respectively, while 60 Pa to 130 Pa and 89.7% to 92.9% for coir fibre material pads respectively under operating air velocities of 2.0 m/s to 3.0 m/s. Franco et al. (2010) tested cellulose evaporative cooling pads in laboratory using a new methodology in a wind tunnel. They recommended a range of air speeds through the pad of 1 to 1.5 m/s, at which the pressure drop was between 3.9 and 11.25 Pa, depending on the type of pad and the water flow applied. The saturation efficiency ranged between 64% and 70%, while the amount of evaporated water varied between 1.8 and 2.62 kg h⁻¹ K⁻¹ per square meter of pad area.

Ruthven (1984) stated that the surface of an adsorbent consists of meso-pores and macro-pores wherein the adsorbate is accumulated. The larger the area

and the number of the pores, the more amount of adsorbate are being accumulated. Pesaran and Bingham (1989) stated that a desiccant cooling system involves passing humid (and warm) air through a desiccant dehumidifier for drying and through a cooler for sensible cooling to provide conditioned air. The desiccant becomes saturated with water and needs to be regenerated with hot air provided by an energy source (e.g., sun, natural gas, waste heat, or electricity). Collier (1989) stated that the cost, efficiency, and durability of a desiccant cooling/dehumidification system depend on those of the components used in the system. The desiccant dehumidifier is a major component in the system. The performance of a desiccant dehumidifier depends strongly on the properties of its desiccant and the geometry of the matrix. According to Liu et al. (2005a, b) and Chen et al. (2010), silica-gel-water is used as working pair and mass recovery-like process is adopted in order to use low temperature heat source ranging from 70 to 85°C effectively. The chiller (1 kg silica-gel) has a cooling capacity of 75 W to 270 W and coefficient of Performance (COP) ranging from 0.2 to 0.42 according to different evaporating temperatures. Compared with other adsorbents, silica-gel can be regenerated at a relatively low temperature, i.e. below 100°C and typically about 85°C. Wang et al. (2005) mentioned that up to now, there have been four chillers to be applied in the real systems such as the solar energy air conditioning system and building cooling, heating and power (BCHP) system. Awad et al. (2008) stated that the dehumidification period increases with decrease in air flow rate and desiccant bed (radial flow and cylindrical shape) diameter ratio. The increase in diameter ratio increases the pressure drop within the bed and rises the bed adsorption capacity for short operation periods. This analysis allows identifying and quantifying the energy losses in the air blowing system for the specified dehumidification capacity of the desiccant bed.

The aforementioned statements, related to livestock housing and greenhouses, justify the need to improve

the design of the traditional evaporative cooling pad systems to enable them to support temperature differences over 15 °C between inside and outside of the barn, thus providing the suitable microclimatic conditions for animal and plant production. This research project aims at prototyping a new desiccant system to be installed on the traditional cooling pads so as not to be negatively affected by high moisture content in the external air, thus enhancing their efficiency. In order to achieve these goals, a hypothesis has been developed to enhance the efficiency of cooling pads. Testing this hypothesis is divided into several phases. This paper represents the first phase and aims at testing the hypothesis in laboratory and provides useful results to be implemented in the next phases.

2 Theoretical considerations

2.1 Hypothesis and statement of research

Installing segments filled with chemical compounds, which are able to adsorb moisture, on the external face of cooling pads will result in adsorbing moisture from external air before entering the cooling pads. This will increase the treated-air ability of absorbing more water from cooling pads, i.e. cooling pads will evaporate more water in the treated air. Water evaporation requires heat energy which will be obtained from the treated air. Hence, the temperature of the treated air will decrease much more than the non-treated air in the traditional cooling pads. This process will increase the efficiency of cooling pads systems. The ASABE Standards (2008a, b, c) were used to select the design parameters of mechanical ventilation systems, ventilation fans and evaporative cooling pads whereas these design parameters were implemented to propose a desiccant system design. Figure 1 shows the proposed design of a desiccant system mounted next to cooling pads and Figure 2 shows the proposed location of the desiccant system on the external face of the cooling pads.

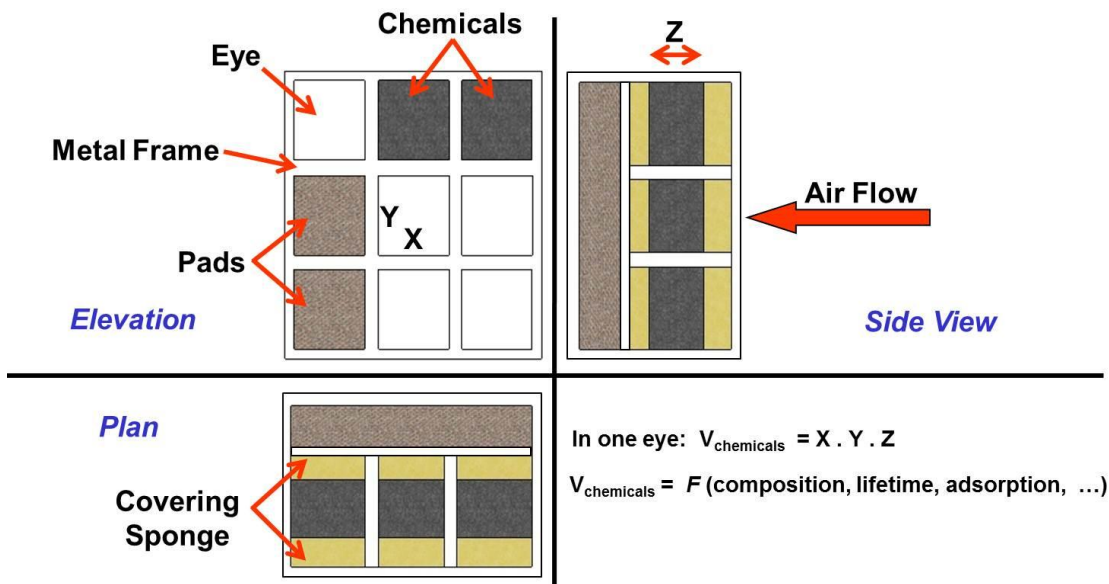


Figure 1 The proposed desiccant system design.

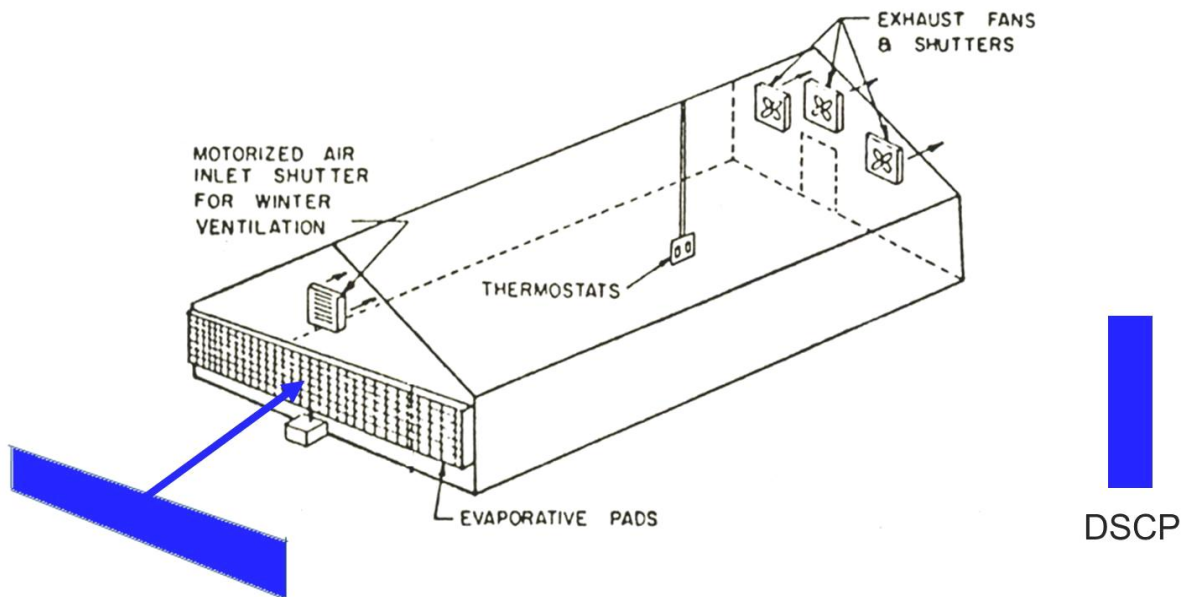


Figure 2 The proposed desiccant system location (changed after Hellickson and Walker, 1983).

In case of animals and plants sensitive to high humidity levels, additional desiccant segments can be installed on the internal face of the cooling pads to reduce the moisture content of the incoming air. The final design shows two columns of desiccant segments, where the first one is installed on the external face of the cooling pads and the second one on the internal face of the cooling pads. Questions concerning costs, static pressure, energy consumption etc. have to be investigated and answered.

3 Materials and methods

211 laboratory experiments were carried out (25 were preliminary tests, 78 in laboratory setup and 30 in a climate chamber). Additionally, 78 reactivation experiments were conducted in drying cabinet. The possibility and effectiveness of using several desiccants to fill the segments was investigated. The following desiccants were used in the investigations to achieve the moisture absorption: ARTSorb™, PROSorb™, Silica Gel, Silica Gel Macro-porous, and a mixture of the

aforementioned desiccants with equal ratios on mass basis. Table 1 shows the physical properties of the abovementioned desiccant materials. The advantages of these desiccants are: inert, cheap, insoluble in reaction

media, and solid. The selection of any of these desiccants depends on its price, availability, reversibility, and efficiency. These compounds were individually tested in specially designed laboratory experiments.

Table 1 The physical properties of different desiccants under consideration (information from the product companies)

Desiccant	Shape	Density	Porosity	Diameter	Dry colour	Wet colour	Reactivation temperature
		/(kg/L)	/(mL/g)	/(mm)			
ARTSorb™	Granular	0.87	2-3	1.5-3	White	White	60
PROSorb™	Granular	0.75	4-5	3-5	Brown	Brown	60
Silica Gel	Granular	0.75	3.2-5	2-5	Blue	Rose	140
Silica Gel Macro-porous	Spherical	0.65	6.5-8	6-10	White	White	140

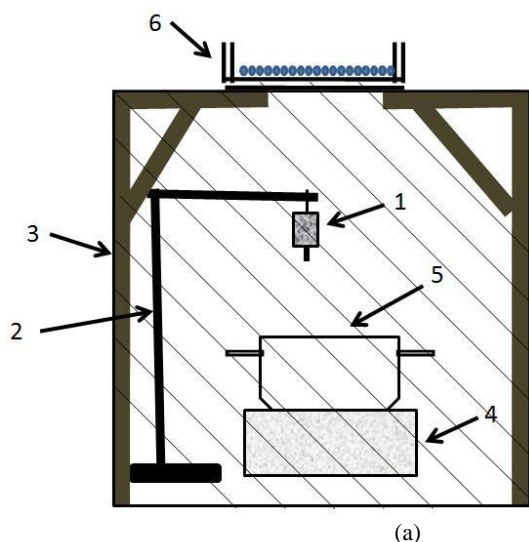
3.1 Experiments

The main experiments of this study were primarily carried out to determine the adsorption capacity and rate, and the regeneration/reactivation behavior, i.e. the desorption process. Therefore, three experimental designs were implemented: laboratory setup, climate chamber and drying cabinet.

3.1.1 Laboratory setup

This laboratory setup was used to measure and analyze the sorption and desorption properties of the different desiccants. It determines how much water can be adsorbed by each desiccant. The determination of

this parameter was carried out in function of time. The results were implemented further to draw conclusions on the adsorption capacity and adsorption rate of each desiccant. The laboratory setup consists of a wooden frame which was covered with plastic wrap, a hot plate (SLK 2, SCHOTT-Geräte GmbH, Germany), laboratory test sieve with a diameter of 20 cm and a mesh size of 1.5 mm, a pot filled with tap water, a support rod and a temperature-humidity sensor (Comark Diligence EV N2003, Comark Limited, Hertfordshire, England). A detailed overview of the laboratory setup is shown in Figure 3.



1.temperature-humidity sensor 2.support rod 3.wood frame covered with plastic foil 4.hot plate 5.pot of water 6.laboratory sieve containing the desiccant material

Figure 3 Laboratory setup

The structure of the experiment was designed so that an air mass movement was generated. The air was coming through the very small cracks as the system was not fully tight, then the air came through the desiccant material in a natural movement, i.e. not controlled. Within this built environment inside the laboratory setup, the temperature and relative humidity (RH) were stabilized in the range of 35 °C -40 °C and 90%-100%, respectively; where under such conditions, the desiccant should be used later (summer with hot humid days). Outside the system, the room temperature and relative humidity of the laboratory were about 20 °C and 40%-50%, respectively. This resulted in a temperature and humidity gradient between the lab room and the laboratory setup, which eventually led to an air mass flow. The mass balance was controlled so that it could only flow to an opening. This opening was located on the upper surface of the test structure. On this opening, the sieve was placed and filled with the desiccant under consideration. This means that all the generated humid air, which would leave the system, must pass through the desiccant. Throughout each experiment, the desiccant mass, the temperature and relative humidity measured within the built environment were measured and recorded.

At least five experiments were conducted for each desiccant to determine the absorption rate and the adsorption capacity of water from the air through each desiccant. The desiccant was fully reactivated in a drying cabinet and equilibrated at room temperature in a desiccator (where it was kept overnight if necessary) before every experiment. The dry desiccant weighed approximately 145 g at the beginning of every experiment. The set of experiments (adsorption) were conducted 3 times with different time length each one is called a phase. Each experiment lasted about 7 h and 10 min (i.e. 430 min) in the first phase of the experiments, 150 min in the second phase and 90 min in the third phase. This was very important to investigate how the desiccant materials will behave through the different

periods and how this will affect the reactivation duration. This led to determine which were the effective and feasible operation periods and the relevant suitable length of reactivations. The desiccant was weighed every 10 min using a balance (LC2200P, Sartorius AG, Germany). The temperature and relative humidity in the built environment were measured and recorded every 10 min.

3.1.2 Climate chamber

A climate chamber (SB222³⁰⁰, Weiss Umwelttechnik GmbH, Germany) was used to carry out the experiments, where a glass pot ($\phi = 18$ cm) containing the desiccant (approx. 145 g) was placed on the balance and all were placed inside the climate chamber (Figure 4). In the climate chamber the experiments were carried out at constant 70% and 80% RH and always at 35°C.



Figure 4 Climate chamber.

The same balance (LC2200P, Sartorius AG, Germany) used in the laboratory setup was also used in the experiments conducted in the climate chamber and connected with cable to a laptop, where the software of the balance was used to automatically record the weighed mass of both the desiccant and the glass pot in an excel file. The mass was weighed and recorded automatically every minute, where each experiment lasted approx. 7 h. Three experiments were conducted for each desiccant to determine the absorption rate and the adsorption capacity of water from the air through each desiccant. The desiccant was fully reactivated in a drying cabinet and equilibrated at room temperature in a

desiccator (where it was kept overnight if necessary) before every experiment. Although the climate chamber was programmed to control the temperature and the relative humidity to predetermined set values, the same temperature-humidity sensor (Comark Diligence EV N2003, Comark Limited, Hertfordshire, England) was used to measure the temperature and the relative humidity inside the chamber, i.e. the surrounding of the desiccant under consideration, every 10 min. This is to detect any malfunctions of the climate chamber during the experiments.

3.1.3 Drying cabinet

The desiccant desorption process, i.e. reactivation process, was carried out in a laboratory drier (MEMMERT UE 400, Memmert GmbH & Co. KG, Germany). Petri palates, lab sieve and glass pot containing the saturated desiccant with moisture, were placed inside the lab drier where the desiccant is reactivated (Figure 5). Furthermore, the same balance was used to determine the desiccant weight loss during the drying/reactivation process which was conducted at a temperature of 140 °C for Silica Gel and Silica Gel Macro-porous, but ARTSorb™ and PROSorb™ were reactivated at a temperature of 60°C. Therefore, the mixture was also reactivated at 60°C. The desiccant was weighed every 10 min outside of the drying cabinet, as this was the only possible method to weigh the material. It was ensured that this step took a max of 30 s to be achieved each time. It is believed that this very short period cannot affect the measurements. The conditions were those of the laboratory (controlled room) which was measured and recorded and were almost fixed at 20°C and 50% RH. Five experiments, each lasting 240 min, were conducted for each desiccant to determine the desorption rate.



Figure 5 Laboratory drier.

3.2 Mathematical modeling

3.2.1 Adsorption

The following mathematical model was developed and used to estimate the water adsorption capacity, δ , (g H₂O/g desiccant) and the water adsorption rate, δ_t , (g H₂O/g desiccant/h):

$$\delta = \frac{W_A}{M_D} \quad (1)$$

$$\delta_t = \frac{W_A}{M_D \times \left(\frac{t}{60}\right)} \quad (2)$$

Where, W_A represents the total amount of adsorbed water by the desiccant (g), M_D is the mass of the dry/active desiccant (g), t designates the duration of the whole experiment (min).

In order to record the variables measured with time throughout the different experiments and compute the dependants; a spreadsheet model was specially developed for this type of experiments. The developed spreadsheet model allows recording the experiment identification (test number and date), the time interval between the measurements within the same experiment (t_i , min), start and end timing of the experiment, the mass of the empty sieve (M_{S_E} , g), mass of the dry desiccant (M_D , g), total dry mass (sieve and dry desiccant) at the start of the experiment (D_T , g), total wet mass (sieve and saturated desiccant) measured from start to end of the experiment (W_T , g), increasing mass of the desiccant with time (I_{M_D} ,

g), desiccant mass difference with time (Δm_A , g) due to water adsorption, sum of adsorbed water with time until the end of the experiment (S_{W_A} , g), total adsorption capacity at the end of the experiment, average adsorption rate, temperature ($^{\circ}\text{C}$) and relative humidity (%) with time inside the controlled environment as well as their averages. The calculations were carried out using the following model:

$$I_{M_D}^n = W_T - M_{S_E} \quad (3)$$

$$\Delta m_A^n = I_{M_D}^n - I_{M_D}^{n-1} \quad (4)$$

$$S_{W_A}^n = S_{W_A}^{n-1} + \Delta m_A^n \quad (5)$$

Where, $S_{W_A}^{n=43}$ is recorded at the end of the experiment, i.e. after 7 h and 10 min with t_I equals to 10 min; therefore, $S_{W_A}^{n=43}$ is equal to W_A which represents the total amount of adsorbed water by the desiccant (g) at the end of the experiment and its value is then substituted in Equations (1) and (2).

On the other hand, the change of adsorption rate with time (C_{δ_i} , g $\text{H}_2\text{O}/\text{g}$ desiccant/min) and the growth of adsorption rate with time (G_{δ_i} , g $\text{H}_2\text{O}/\text{g}$ desiccant/min) were used to draw the relevant curves. Therefore, they were calculated as follows:

$$C_{\delta_i}^n = \frac{\Delta m_A^n}{M_D \times t_I} \quad (6)$$

$$G_{\delta_i}^n = G_{\delta_i}^{n-1} + C_{\delta_i}^n \quad (7)$$

In order to understand how the desiccant functions, it is essential to determine the equilibrium moisture content (EMC). The quantity of moisture in a desiccant material that adsorbs water depends on the temperature and relative humidity of the surrounding air. If the temperature or relative humidity changes, then the moisture content within the desiccant changes which leads it into equilibrium with the new conditions of the

surrounding air. The EMC (%) can be estimated using the following equation:

$$EMC = \left(\frac{I_{M_D}^n - I_{M_D}^{n-1}}{I_{M_D}^n} \right) \times 100 \quad (8)$$

Where, moisture content is the weight of water in the desiccant expressed as a percentage of its dry weight. The EMC is the moisture content of the desiccant in equilibrium with a specified relative humidity (RH).

3.2.2 Desorption

A mathematical model was developed and used to calculate the moisture mass loss rate from the saturated desiccant as well as the change of the saturated desiccant mass in function of time. In order to implement the developed mathematical model, a special spreadsheet model was developed wherein the mathematical model was embedded. Within the spreadsheet model the following information were recorded: the experiment identification (test number and date), the time interval between the measurements within the same drying experiment (T_{DI} , min), starting and ending time of the experiment, the drying temperature ($^{\circ}\text{C}$), saturated desiccant mass (D_{M_D} , g) where this mass at the beginning of the drying/reactivation process is equal to saturated desiccant mass at the end of the adsorption experiment and is decreasing with time through the desorption process, the mass of the empty Petri plate (M_{P_E} , g), total wet mass of sieve and wet desiccant (W_T , g), total dry mass of sieve and dry desiccant (D_T , g), desiccant mass difference with time (Δm_D , g) due to desorption, and the sum of the relinquished water (R_W , g) with time. The calculations were accomplished using the following mathematical model:

$$D_{M_D}^n = D_T - M_{P_E} \quad (9)$$

$$R_W^n = D_{M_D}^n - D_{M_D}^{n=0} \quad (10)$$

$$\Delta m_D^n = D_{M_D}^n - D_{M_D}^{n-1} \quad (11)$$

3.2.3 Design parameters

The following mathematical model was developed to implement the results of the laboratory experiments in assessing the design parameters of the desiccant system that is intended to be installed on the cooling pads of full-scale barns. In order to implement the developed mathematical model, a special spreadsheet model was developed wherein the mathematical model was embedded. As the required input data are inserted into the spreadsheet, the output data are displayed automatically. The ASABE Standards (2004; 2008a, b, c) were used to select the design parameters of the different livestock barns and the greenhouse as well as the mechanical ventilation systems, ventilation fans and evaporative cooling pads; where these design parameters were implemented to carry out the theoretical calculations.

The volumetric adsorption rate (\dot{g}_t , m³ air/kg desiccant/h) of the desiccant can be calculated as follows:

$$\dot{g}_t = \frac{\delta \times \mathfrak{R}}{W_C} \quad (12)$$

Where, \mathfrak{R} represents the interval of desiccant reactivation (h⁻¹), and W_C is the water content (kg water/m³ air). The water content is equal to the humidity ratio (g water per g dry air) divided by the specific volume (m³ / kg dry air), where both are determined at specific relative humidity (%) and dry-bulb temperature (°C) using the psychrometric charts. The required quantity of desiccant (χ_{M_D} , kg; V_{M_D} , m³) to fill the segments that will be installed on cooling pads of full-scale barns, can be calculated as follows:

$$\chi_{M_D} = \frac{V_R}{\dot{g}_t} \quad (13)$$

$$V_{M_D} = \frac{\chi_{M_D}}{\rho_{M_D}} \quad (14)$$

Where, ρ_{M_D} represents the density of the desiccant (kg/m³), and V_R is the ventilation rate through the barn (m³/h). The ventilation rate was considered equal to 720 m³/h cow or 6 m³ h⁻¹ bird⁻¹ in summer (Hattem, 1993).

Additionally, ASABE Standards (2008a) stated that the required ventilation rate for swine housing is 4.7 × 10⁻² m³ s⁻¹ sow⁻¹ (68-95 kg live weight) in summer. The abovementioned ventilation rates are maximum ventilation rates which are considered for summer seasons and should be multiplied by the number of cows, birds or pigs housed in the barn, respectively; in order to get the ventilation rate through the barn (V_R). On the other hand, ASABE Standards (2008b) stated that evaporative cooling capacity is 0.08 m³ s⁻¹ m⁻² of floor area. The estimated quantity of the required desiccant can then be used to calculate its price, where the market price for tonnage quantities is 2.6 €/kg. The thickness of the desiccant segments (τ_{DS} , m) that will be installed on cooling pads of full-scale barns, can then be calculated as follows:

$$\tau_{DS} = \frac{V_{M_D}}{A_P} \quad (15)$$

Where, A_P is the face area of the cooling pads (m²). The pads face area is equal to the pads height, 0.5-2.5 m (Wiersma and Short, 1983), multiplied by the length of the barn side where the pads are installed as either barn length or width.

The calculations related to the fan(s) were carried out as stated in the literature (Hellickson and Walker, 1983; Albright, 1990; Hattem, 1993; Lindley and Whitaker, 1996). These calculations are applicable to the fan(s) required to operate the system in a full-scale barn as well as in the proposed lab-scale model (see section 7.1). The static pressure (P_S , Pa) of the required fan(s) can be calculated as follows:

$$P_S = P_{fr} + P_V + \Delta P \quad (16)$$

Where, P_{fr} represents the friction losses (Pa), P_V is the velocity pressure (Pa), and ΔP is the pressure drop (Pa). These resistances are caused by cooling pads. The friction losses can be calculated using Darcy-Weisbach Equation:

$$P_{fr} = \left(\frac{f}{D} \right) \times L \times \left(\frac{V^2}{2g} \right) \quad (17)$$

Where, f represents the friction factor, D is the duct diameter (m), L is the duct length (m), V is the air velocity (m/s) through the duct, and g is the gravity acceleration (m/ s²). The velocity pressure can be calculated as follows:

$$P_V = \rho \left(\frac{V}{1097} \right)^2 \quad (18)$$

Where, ρ represents the air density (kg/m³). The pressure drop can be calculated as follows:

$$\Delta P = \Delta P_{DS} + \Delta P_{CP} \quad (19)$$

Where, ΔP_{CP} is the pressure drop (Pa) through the cooling pads and its value is provided subject to the pads' material by the references (Wiersma and Short 1983; Koca et al., 1991; Liao et al., 1998), and ΔP_{DS} is the pressure drop (Pa) through the desiccant segments and can be calculated as follows (Daragan et al., 1979):

$$\Delta P_{DS} = \tau_{DS} \times \xi \times \left(\frac{2 \times \rho \times V^2}{d} \right) \quad (20)$$

Where, ξ represents the drag coefficient, and d is bead size, i.e. the bead diameter of the desiccant material (m). On the other hand, the porous wall thickness which represents the thickness of the desiccant segments (τ_{DS}) is substituted in this equation in meters.

The electrical power (P_{el} , kW/m²) per unit area of the pads-segments required to operate the fan(s) can be calculated as follows:

$$P_{el} = \frac{\Delta P \times Q}{3600 \times \left(\frac{\eta}{100} \right)} \quad (21)$$

Where, Q (m³/m² h) is the volumetric flow rate per unit area of the pads-segments, and η (%) is the efficiency. The electrical energy (E_{el} , kWh m⁻² month⁻¹) per unit area of pads-segments and month can be calculated as follows:

$$E_{el} = P_{el} \times D_O \times 30 \quad (22)$$

Where, D_O (h/d) represents the operating duration of the system which was considered equal to 12 h per day.

Ultimately, the variable costs (C_V , Currency m⁻² month⁻¹) can be calculated as follows:

$$C_V = E_{el} \times C_{el} \quad (23)$$

Where, C_{el} (Currency k/Wh) is the cost of one kWh and was considered equal to 0.2 € /kWh according to the European market prices.

4 Results

The results of the experiments carried out in the laboratory setup, climate chamber and drying cabinet as well as the results of the theoretical calculations are presented as average values in various tables and figures.

4.1 Laboratory setup

Tables 2, 3 and 4 show the results of the experiments conducted in the laboratory setup through the first, second and third phase, respectively. The experiments were carried out at 35 -40°C and 90% -100% RH. Figure 6 shows the growth of adsorption rate with time for the different desiccants under consideration at 35 -40°C and 90%-100% RH in the laboratory setup. Figure 7 shows the change of adsorption rate with time for the different desiccants under consideration at 35 -40°C and 90% -100% RH in the laboratory setup.

Table 2 Results (averages) of the first phase of the laboratory setup at 35-40 °C and 90%-100% RH, where each

experiment lasted 430 min					
Desiccant	Number of experiments	δ	δ_t	C_{δ_t}	EMC
ARTSorb™	5	125	17	0.29	12.5
PROSorb™	5	158	22	0.37	15.8
Silica Gel	8	257	36	0.6	25.7
Silica Gel Macro-porous	5	132	18	0.31	13.2
Mixture	5	142	20	0.33	14.2

Note: δ represents water adsorption capacity (g H₂O/ kg desiccant); δ_t represents water adsorption rate (g H₂O/(kg desiccant h)); C_{δ_t} represents change of adsorption rate with time (g H₂O/ (kg desiccant min)); EMC represents equilibrium moisture content (%), at 90-100% RH.

Table 3 Results (averages) of the second phase of the laboratory setup at 35-40 °C and 90%-100% RH, where each experiment lasted 150 min

Desiccant	Number of experiments	δ	δ_t	C_{δ_t}	EMC
ARTSorb™	5	52	21	0.35	5.2
PROSorb™	5	80	32	0.53	8

Silica Gel	5	111	44	0.74	11
Silica Gel Macro-porous Mixture	5	75	30	0.50	7.5
Mixture	5	53	21	0.35	5.3

Desiccant	Number of experiments	δ	δ_t	C_{δ_t}	EMC
ARTSorb TM	5	32	21	0.36	3.2
PROSorb TM	5	49	33	0.54	4.9
Silica Gel	5	62	41	0.69	6.2
Silica Gel Macro-porous	5	55	37	0.61	5.5
Mixture	5	30	20	0.33	3

Table 4 Results (averages) of the third phase of the laboratory setup at 35-40 °C and 90-100% RH, where each experiment lasted 90 min

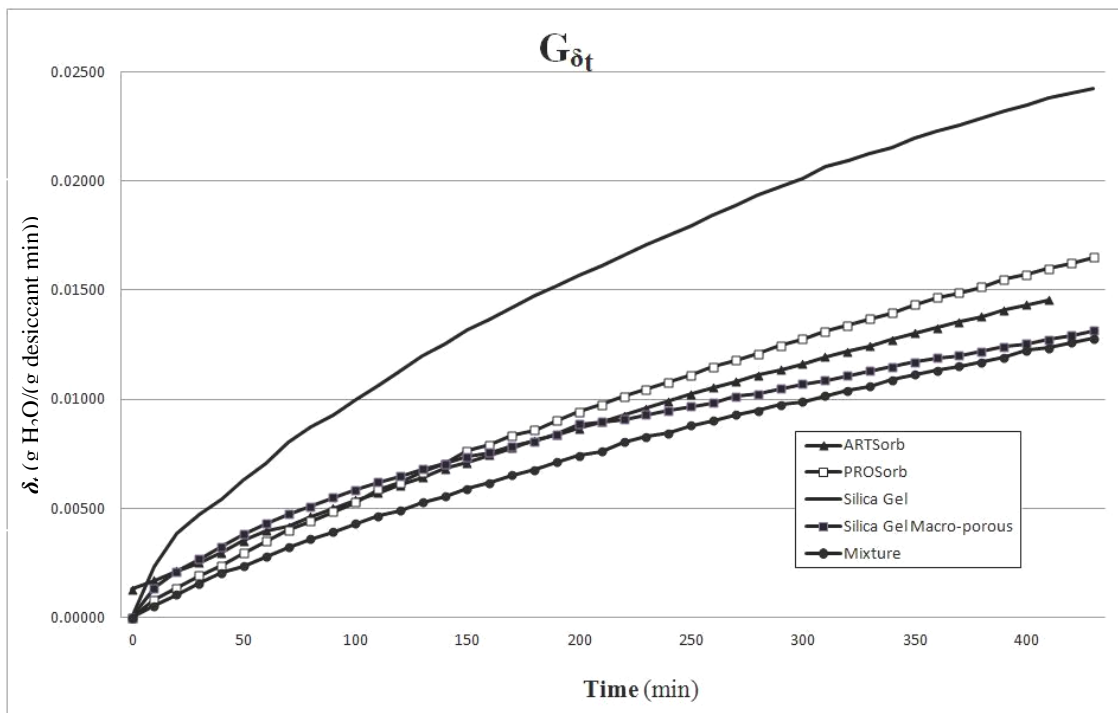


Figure 6 Growth of adsorption rate with time for the different desiccants under consideration at 35-40 °C and 90%-100% RH in the laboratory setup through 430 min.

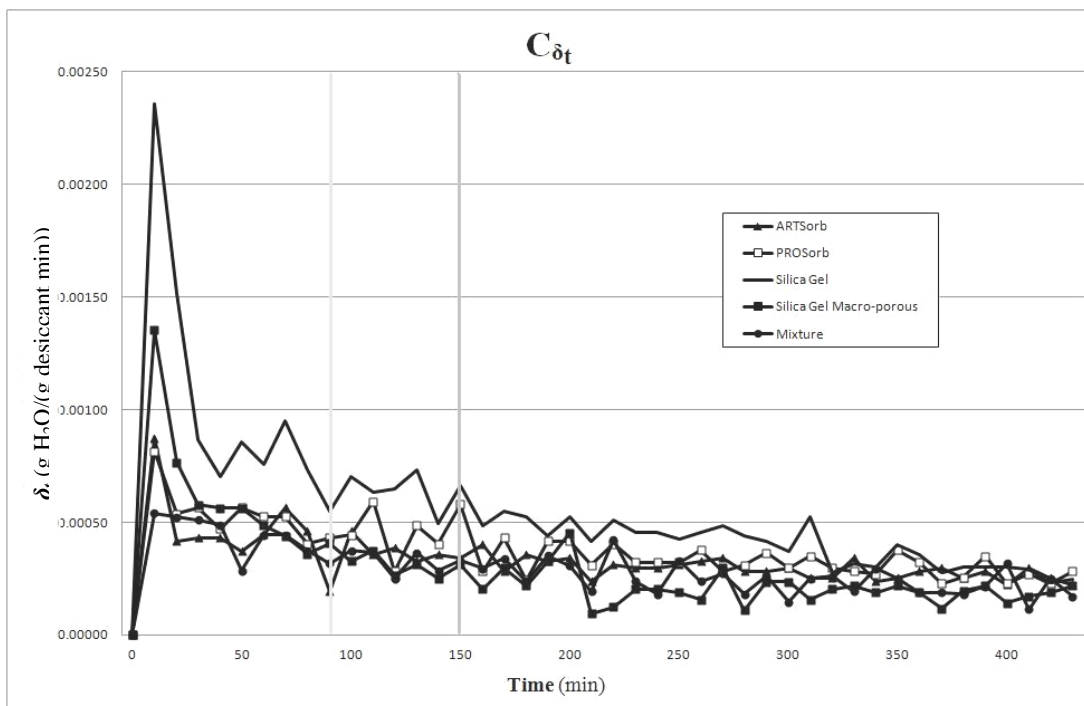


Figure 7 Change of adsorption rate with time for the different desiccants under consideration at 35 -40°C and 90% - 100% RH in the laboratory setup through 430 min.

4.2 Climate chamber

Table 5 and Table 6 shows the results of the experiments conducted in the climate chamber at 35°C and 80% RH, and at 35°C and 70% RH, respectively. Figure 8 and Figure 9 show the growth of adsorption rate with time for the different desiccants under consideration at 35°C and 80% RH, and at 35°C and 70% RH, respectively. Figures 9 and 10 show the change of adsorption rate with time for the different desiccants under consideration at 35°C and 80% RH, and at 35°C and 70% RH, respectively.

Table 5 Results (averages) of the experiments conducted in the climate chamber at 35°C and 80% RH

Desiccant	Number of experiments	δ	δ_t	C_{δ_i}	EMC
ARTSorb™	3	75	11	0.19	7.5
PROSorb™	3	100	14	0.25	10
Silica Gel	3	137	20	0.4	14
Silica Gel Macro-porous	3	58	8.3	0.14	5.8
Mixture	3	72	10.2	0.18	7.2

Table 6 Results (averages) of the experiments conducted in the climate chamber at 35 °C and 70% RH

Desiccant	Number of experiments	δ	δ_t	C_{δ_i}	EMC
ARTSorb™	3	89	13	0.22	8.9
PROSorb™	3	116	17	0.29	11.6
Silica Gel	3	123	18	0.3	12.3
Silica Gel Macro-porous	3	56	8	0.14	5.6
Mixture	3	68	9.3	0.17	6.6

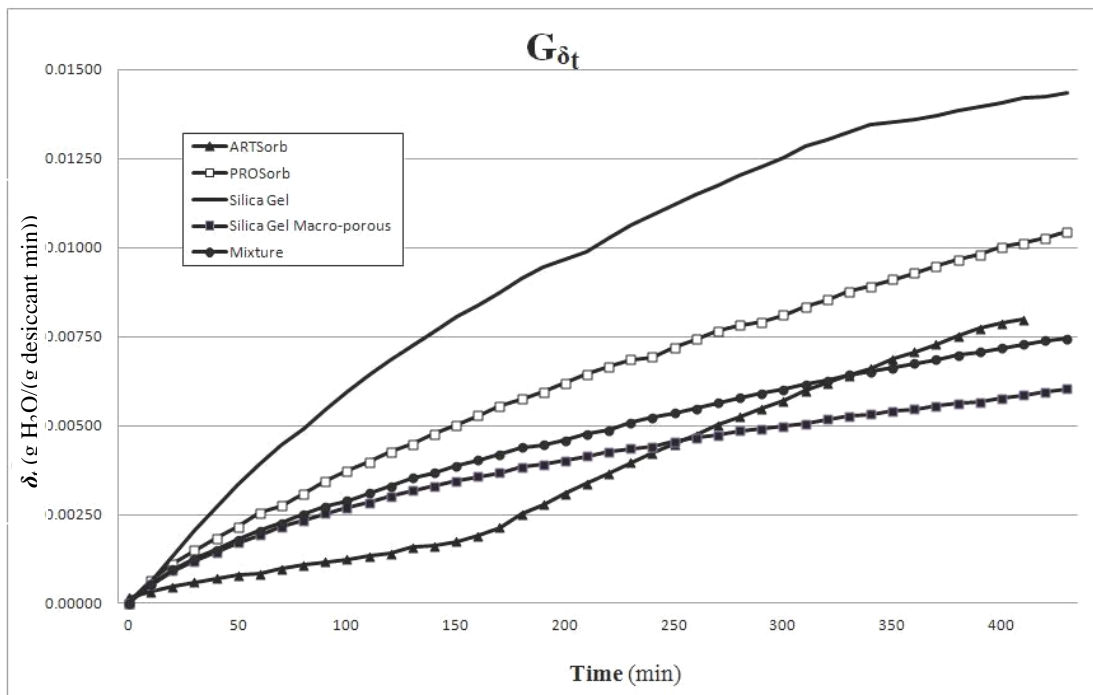


Figure 8 Growth of adsorption rate with time for the different desiccants under consideration at 35 °C and 80% RH in the climate chamber through 430 min

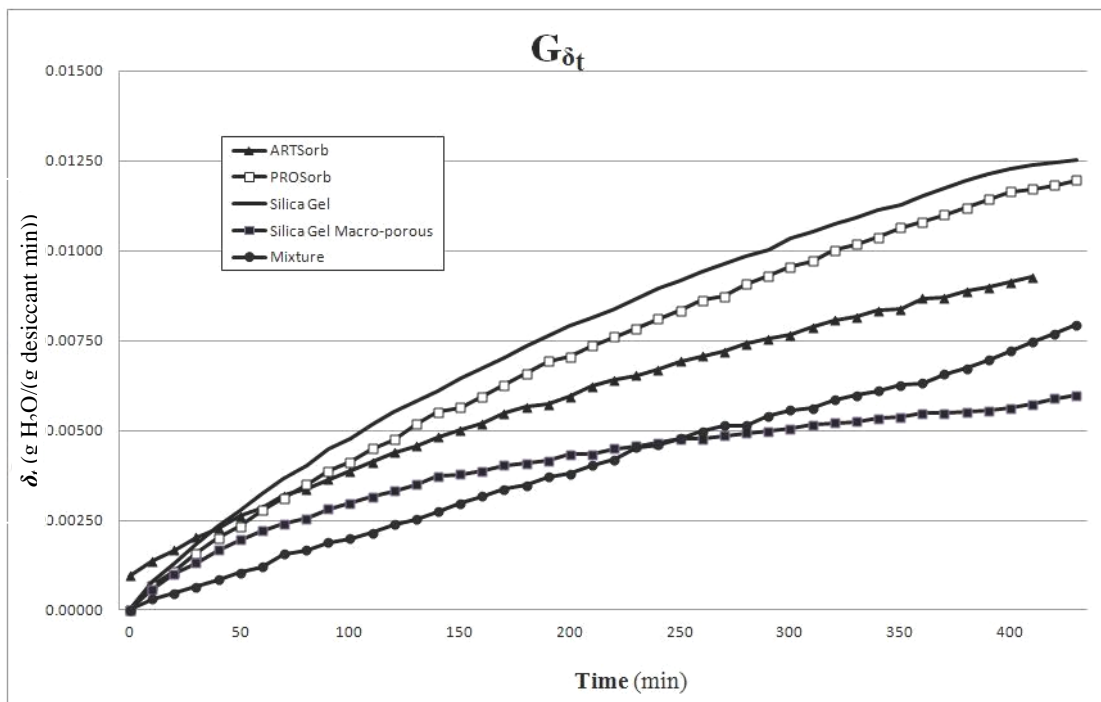


Figure 9 Growth of adsorption rate with time for the different desiccants under consideration at 35 °C and 70% RH in the climate chamber through 430 min

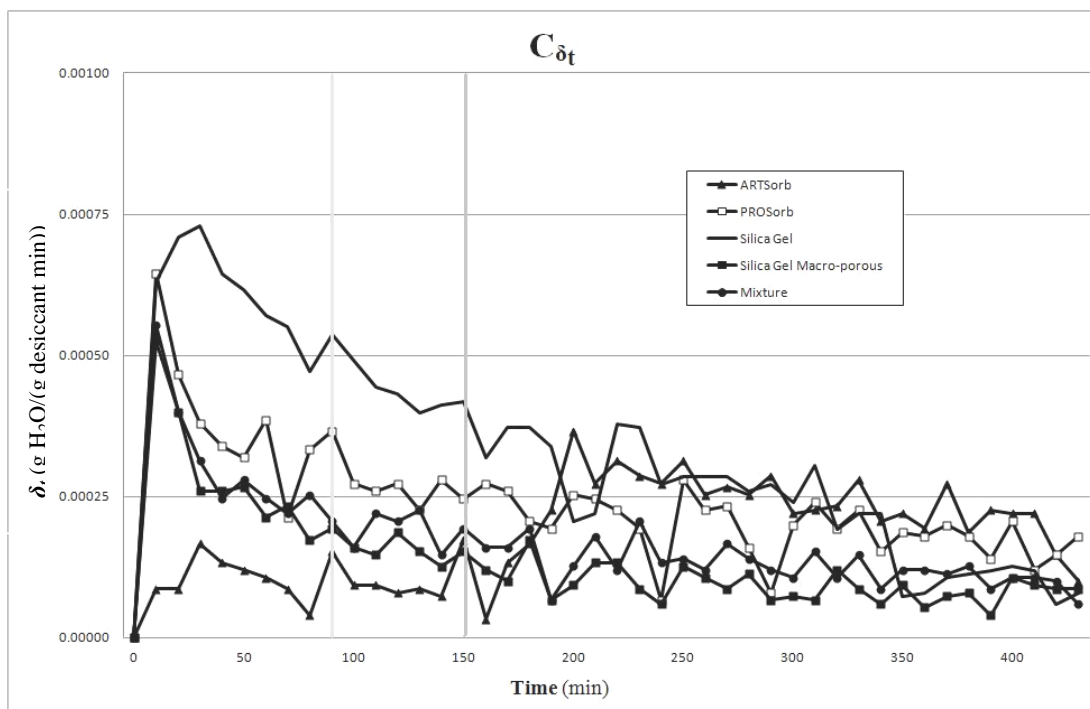


Figure 10 Change of adsorption rate with time for the different desiccants under consideration at 35 °C and 80% RH in the climate chamber through 430 min

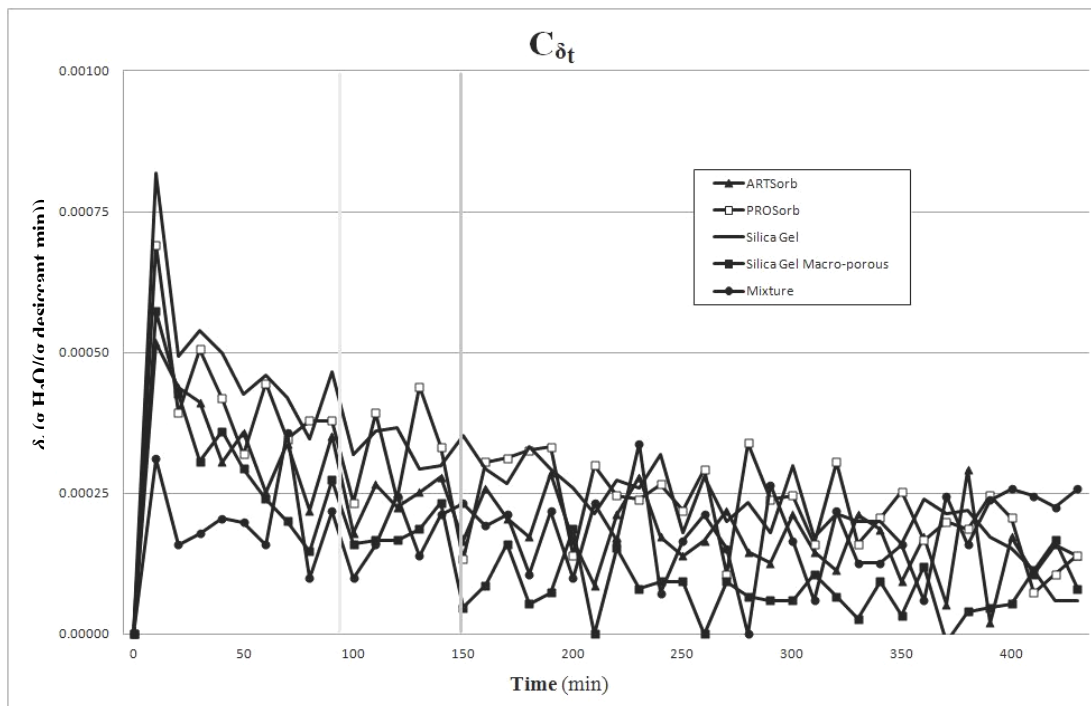


Figure 11 Change of adsorption rate with time for the different desiccants under consideration at 35 °C and 70% RH in the climate chamber through 430 min

4.3 Drying cabinet

Figures 12, 13 and 14 show the mass change with time for the different desiccants under consideration through desorption/reactivation process after the first, second and third phase of sorption, respectively.

Figures 15, 16 and 17 show the profiles of mass loss with time for the different desiccants under consideration through desorption/reactivation process after the first, second and third phase of sorption, respectively.

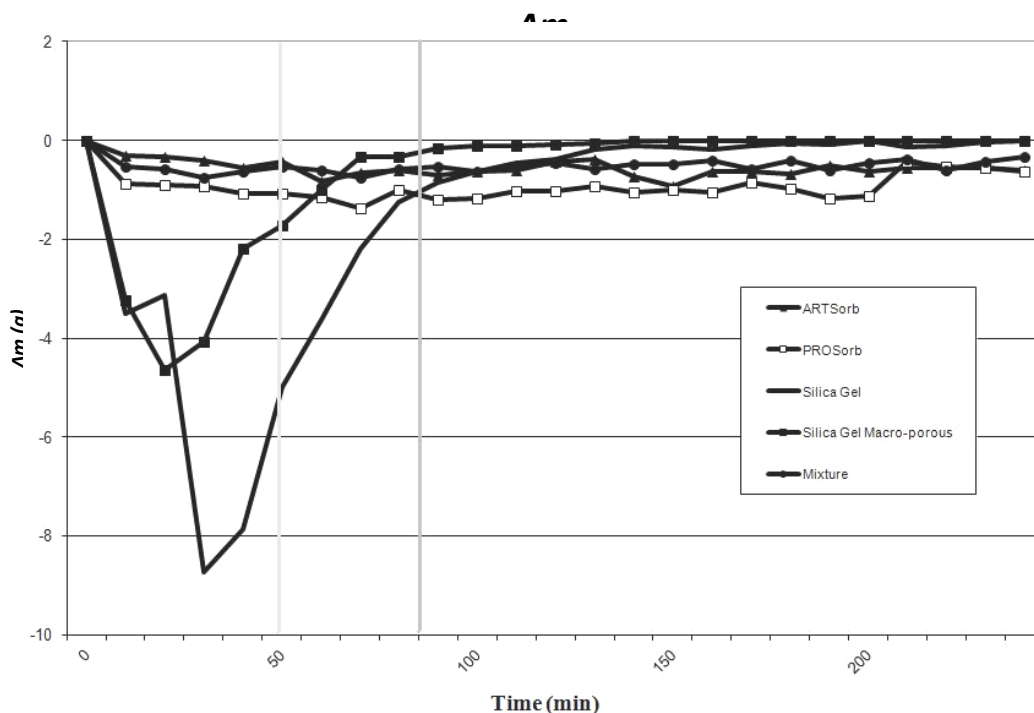


Figure 12 Mass change with time (240 min) for the different desiccants under consideration through the desorption/reactivation process after the first phase of sorption

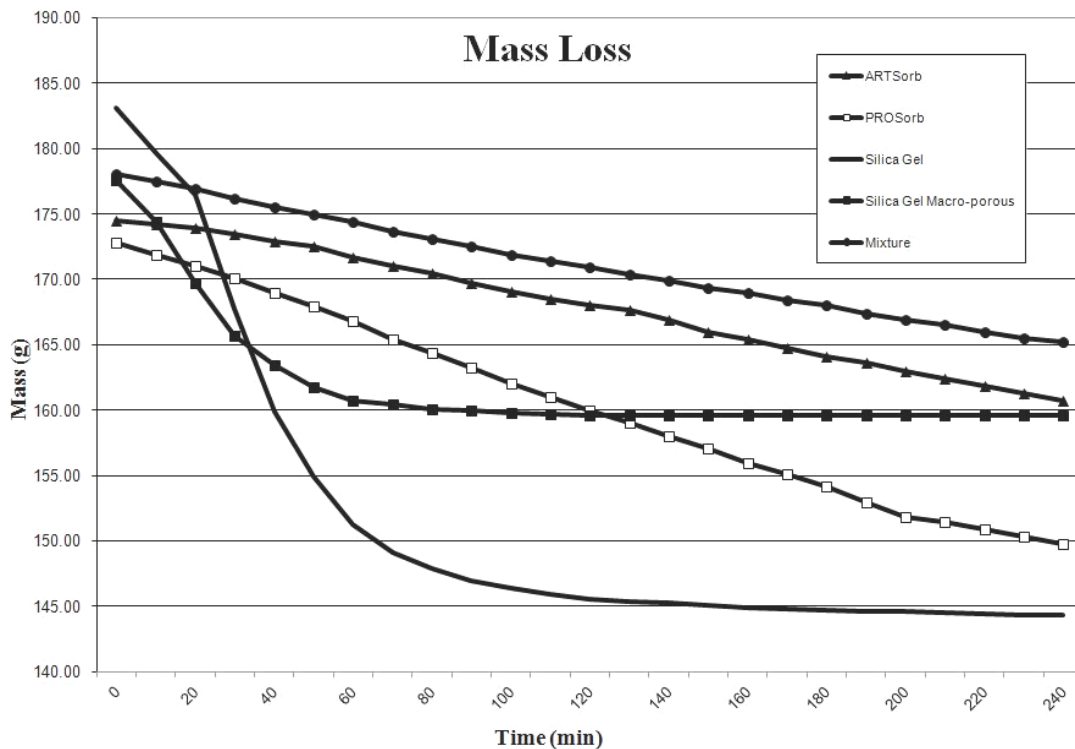


Figure 15 Mass loss with time (240 min) for the different desiccants under consideration through the desorption/reactivation process after the first phase of sorption

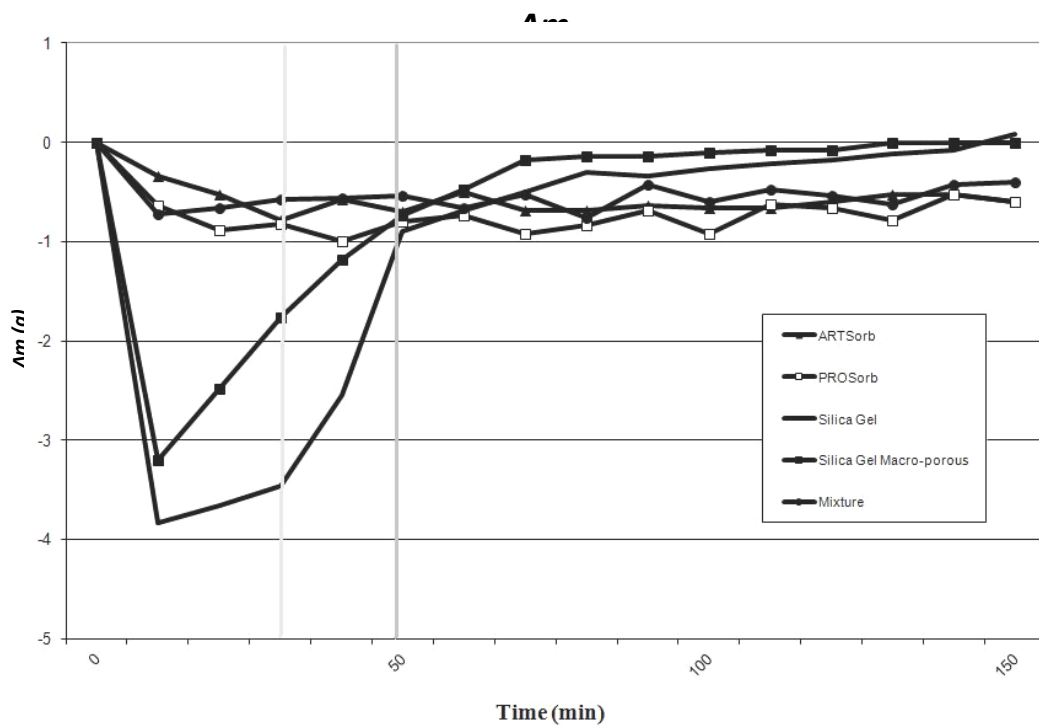


Figure 13 Mass change with time (150 min) for the different desiccants under consideration through the desorption/reactivation process after the second phase of sorption

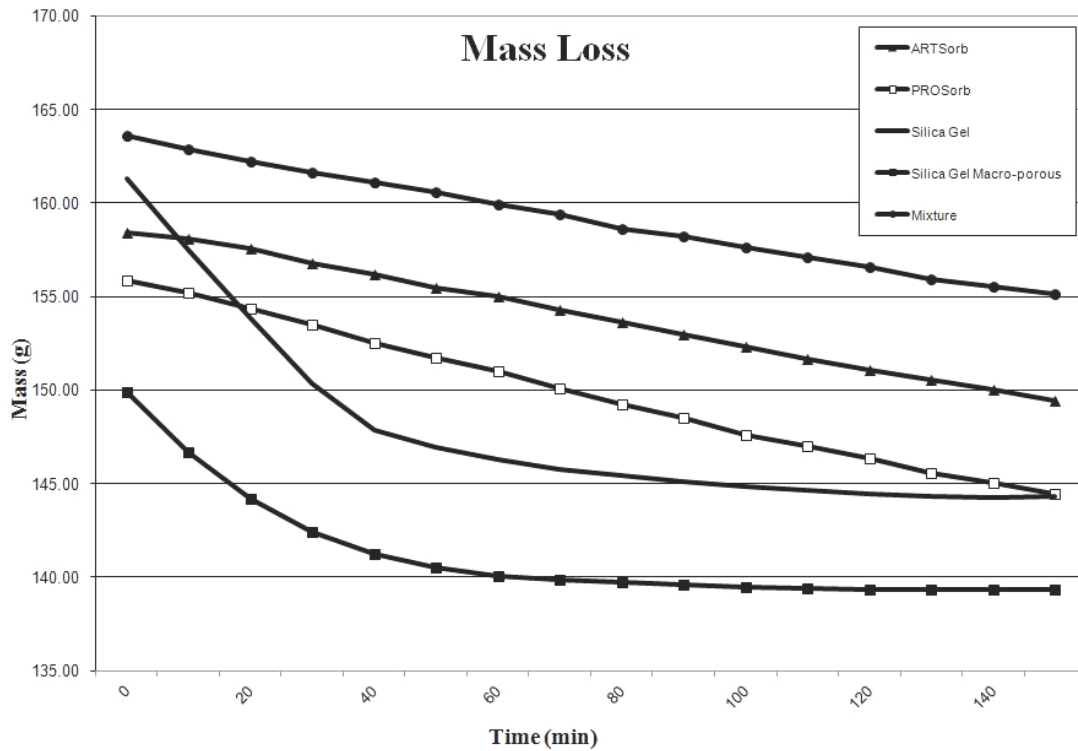


Figure 16 Profiles of mass loss with time (150 min) for the different desiccants under consideration through the desorption/reactivation process after the second phase of sorption

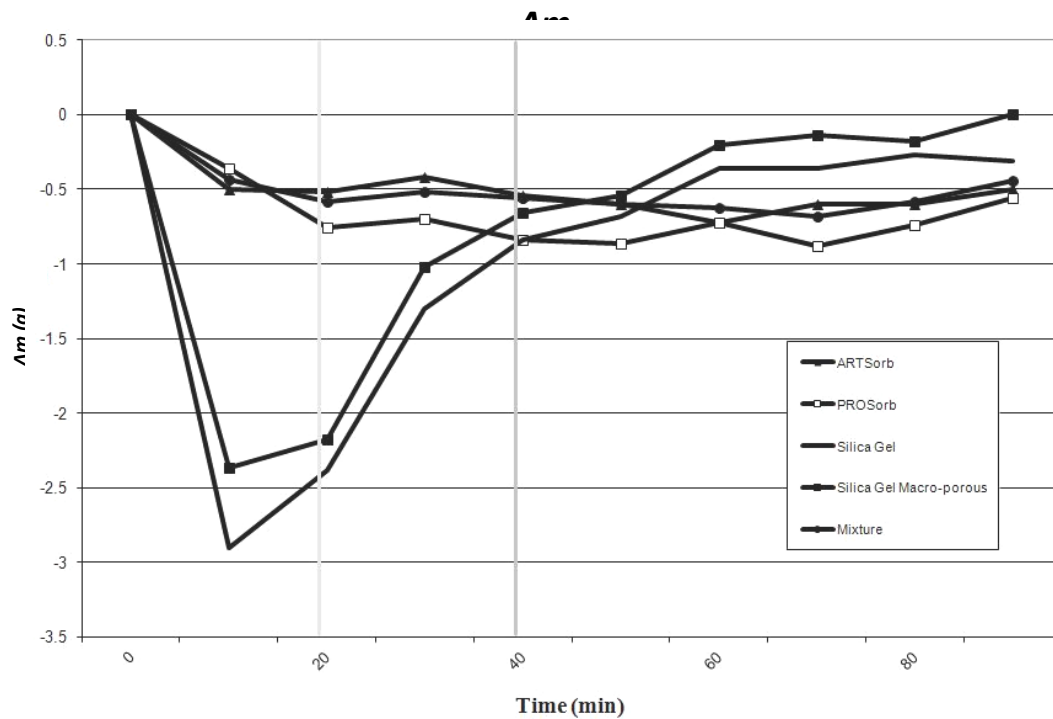


Figure 14 Mass change with time (90 min) for the different desiccants under consideration through the desorption/reactivation process after the third phase of sorption

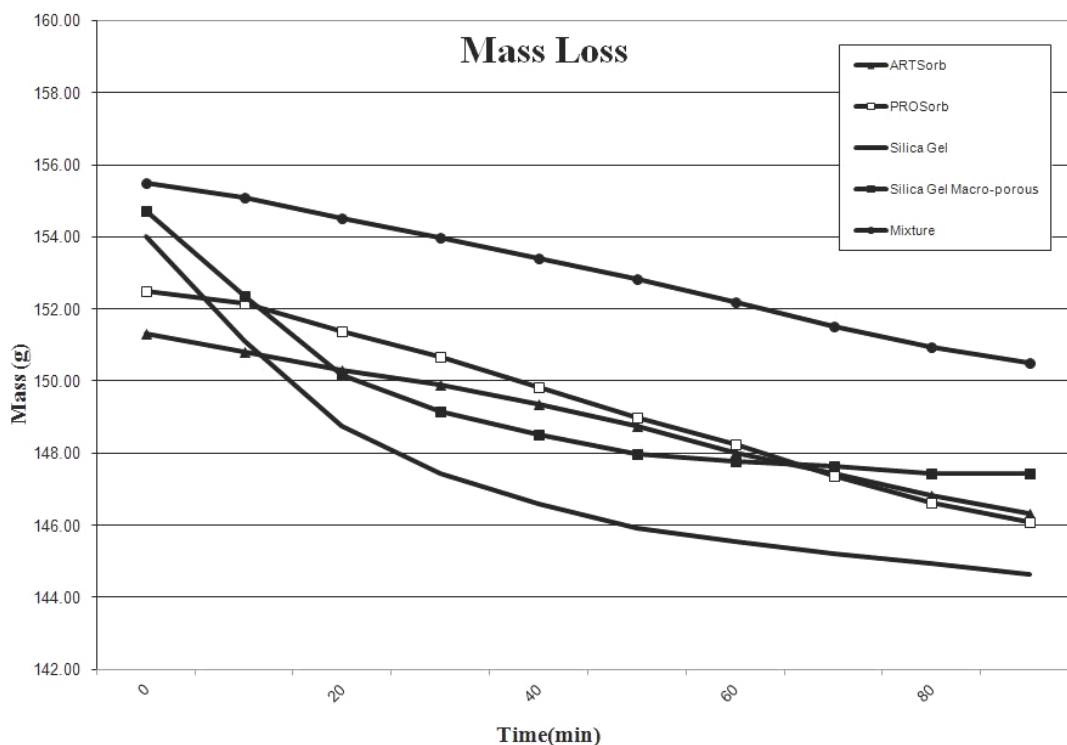


Figure 17 Profiles of mass loss with time (90 min) for the different desiccants under consideration through the desorption/reactivation process after the third phase of sorption

4.4 Theoretical calculations

Tables 7 and 8 show the results of the theoretical calculations and the expected enhancement of the cooling system efficiency under various conditions. Table 7 shows the size of the desiccant system (area, thickness),

required quantity of desiccant, pressure drop, electricity consumption and costs. Table 8 shows the enhancement to the cooling system efficiency under various conditions based on temperature and relative humidity.

Table 7 Results of the theoretical calculations: size of the desiccant system, quantity of desiccant, pressure drop, electricity consumption and costs

Factor	Dairy housing	Poultry housing	Swine housing	Greenhouse
Number of animals housed in the barn	110	30,000	570	-
Size (m ²)	-	-	-	460
Area of pads/segments (m ²)	70	160	80	120
Thickness of desiccant segment (cm)	10			
Operating duration (h)	12			
Desiccant volume (m ³)	7	16	8	12
Desiccant mass (Ton)	4.9	11.2	5.6	8.4
Desiccant mass per unit area of pads (kg/m ²)	70			
Total price of desiccant, i.e. fixed costs (€×10 ³)	12.7	29.1	14.6	21.8
Total pressure drop(kPa)	0.6			
Power per unit area(kW m ⁻²)	0.18			
Electrical energy per unit area(kWh m ⁻² month ⁻¹)	63.5			
Costs of electricity consumption (€ m ⁻² month ⁻¹)	12.7			
Variable costs(€/month)	889	2032	1016	1524

Table 8 Enhancement to the cooling system efficiency under various conditions (Case 1 – 6)

Case	Temperature (°C)	Relative humidity (%)	Water content (kg water/m ³ air)	Enhancement percentage (%) ^a			
				Dairy	Poultry	Swine	Greenhouse
1	25	50	0.010	38	28.5	26.6	29.1
2	35	50	0.020	19	14.3	13.3	14.5
3	35	60	0.025	15.2	11.4	10.7	11.6
4	35	70	0.028	13.6	10.2	9.5	10.4
5	35	80	0.033	11.5	8.6	8.1	8.8
6	35	90	0.038	10	7.5	7	7.7

Note: ^a The results presented in this table were based on the model calculations elucidated in Eqs. 3, 8, 12, 13, 14 and 15.

5 Discussion

In this study, the experiments were conducted to investigate the possibility of implementing desiccant materials for developing a desiccant system to adsorb moisture from outdoor air before introducing it into the cooling pads. These desiccant materials are usually used for static applications, e.g. packs/packets of electrical devices. This study provides new information on dynamic applications for the desiccant materials which were implemented in the experiments carried out in the laboratory setup, climate chamber and drying cabinet, wherein the air was in dynamic motion. A keystone is that the experiments were designed in a manner to approximately simulate the dynamic behavior of air through the pads in practice. An important issue is how the air within the experiments was dynamic, i.e. the air surrounding the desiccant material was in dynamic motion and exchangeable with external air. Actually, in the climate chamber there was a fan (Figure 4) which removes the old-age air from the chamber and allows introducing fresh air with the preset conditions of humidity and temperature. This is understandable for a climate chamber, but through the laboratory setup there was no fan where this process occurred due to natural forces. In the built environment inside the laboratory setup, the temperature ranged between 35 and 40°C and the relative humidity ranged between 90% and 100%. On the other side, the laboratory room temperature ranged between 20 and 25°C and the relative humidity ranged between 45% and 50%. Taking into

consideration that there was a hole at the top of the structure of the laboratory setup where the sieve that contains the desiccant material was located, the temperature difference between the built environment and the laboratory room forced an air exchange between both spaces the lab room and the built environment. The general concept that temperature difference between two spaces creates air exchange between both spaces, was stated by Albright (1990), Hellickson and Walker (1983) and Sallvik (1999). Additionally, the humidity content difference between the lab room and the build environment led to creating equilibrium between both spaces through mass transfer. The concept of this mode of mass transfer was stated by Baehr and Stephan (2006).

In the experiments, the quantity of the used desiccant material was approximately 145 g which provided a maximum of two strata of the desiccant material in the used sieve and glass pot in the experiments. This was predetermined in the pilot experiments, where it was noticed that when making more than two strata the desiccant material was not fully depleted in the sorption process and was clearly noticed when Silica Gel was used, which colour is blue when dry and rose when wet, a significant quantity of Silica Gel remained blue after the sorption process is finished, i.e. not depleted. On the other hand, one strata is a few quantity which may allow inaccurate weighing in the balance, where the target was to determine the mass difference through the desorption and sorption processes with time and this mass difference is small when measured every minute. Therefore, two

strata are optimal. This will be solved using a powerful fan equipped with solar cells to save energy, where the reactivation lasts for a max of 80 min daily as some desiccants require 45-50 min and others require 80 min. The regeneration/reactivation is planned to be achieved automatically and using a solar system to save energy.

Another issue is that a mixture was made among all desiccant materials with equal ratios and tested as a standalone material. The purpose was that each desiccant requires specific conditions of temperature and relative humidity, where it provides the highest adsorption capacity, i.e. the highest performance. These optimal conditions differ from desiccant to another. Therefore, a mixture of all desiccants was made to cover various conditions of temperature and humidity.

Notwithstanding the above, some other desiccant materials were tested through the pilot experiments and are not listed in this study, owing to the fact that these desiccants were inappropriate for the intended application. For instance, the texture and structure of some of the excluded desiccants from this study changed through the sorption process, e.g. Luquasorb changed from solid state to liquid through the sorption process and then shows rheological behaviour which is not suitable for the intended application. Based on the above, the desiccant material should be stable and its solid state should remain unchangeable.

On the other hand, a temperature-humidity sensor/logger was located inside the built environment of the laboratory setup as well as inside the climate chamber in order to detect any malfunctions which affected the results, where some problems were detected and the defected experiments were excluded and entirely repeated. Although the climate chamber had a temperature and humidity controller which is used to preset the required values but cannot record the data over a specific period, some malfunctions were detected due to personal mistakes such as: not filling the water container of the climate chamber, setting wrong values or misdealing with the control program. Such mistakes were first detected

when the temperature and humidity data recoded by the sensor/logger were checked; looking for the causes led to the abovementioned mistakes. All defected experiments were excluded and repeated.

The experiments, conducted in the first phase of the laboratory setup, lasted more than 7 h in order to allow enough time to investigate the adsorption rate (Table 2 and Figure 6). When the first phase was completed, it was noticed that most of the adsorption capacity was attained after a relatively short period which ranged between 90 min and 150 min (Figure 7), where these time lengths were marked with gray lines. Therefore, two additional laboratory phases were launched which implemented the same methodology and laboratory setup but through shorter time lengths, 150 min and 90 min. The results showed that one half of the adsorption capacity is reachable after 150 min (Tables 2 and 3) and this suggested that the desiccant should be reactivated every 150 min (i.e. \mathfrak{R} is equal to 0.4/h) in the future implementation of the desiccant system for cooling pads. However, less than one quarter to one fifth of the adsorption capacity is reachable after 90 min. On the other hand, through the pilot experiments of the desorption process the desiccant was left for a long period in the drying cabinet, where the desiccant was fully reactivated and the mass difference reached almost zero after 220 min up to a maximum of 240 min. Therefore, the desorption/reactivation experiments were designed to allow 240 min for fully reactivating the desiccants and this is shown in Figure 12. Generally, the reactivation period was highly dependent on the type of desiccant. On the other hand, when the desiccant materials were implemented in sorption processes of 150 min, they required 40 min to effectively get rid of most of the moisture and just 25 min to get rid of more than 75% of the moisture which leads to the suggestion that the reactivation in the future implementation of desiccant materials in desiccant segments with cooling pads should last 25 min (Figure 14), but this must be further investigated in lab-scale model and barn model to

minimize this long time to 5-10 minutes which might be achievable through allowing higher volumetric flow rate of hot air driven from a specially reactivation system. A glimmer of hope is shown in Figure 16, where 15 min were enough to get rid of more than 75% of the moisture, but after the third phase of the laboratory setup, i.e. desiccant materials were gone through a sorption process with a time length of 90 min. Generally, through a short period of the desorption process; most of the moisture is desorbed. This can be attributed to the fact that the portions of water which are not strongly bounded within the meso-pores and the macro-pores of the desiccant material and form the largest mass of the adsorbed water are first desorbed and before the strongly bounded water. The generally physical concepts were stated by Ruthven (1984) and Grathwohl (1998). An important outcome is that when the time length of the sorption process was minimized through the different phases of the laboratory setup, the time lengths of the relevant desorption/reactivation experiments dramatically decrease (Tables 2- 4; Figures 12, 14 and 16).

In the laboratory setup it was not possible to stabilize the temperature and the relative humidity; therefore the temperature and the relative humidity were fluctuating in a range of 35 -40°C and 90%-100%, respectively. It was not possible to reach a constant 90% RH or higher in the climate chamber; therefore, the laboratory setup was important to study the adsorption capacity at 90% RH and higher. In the climate chamber the experiments were carried out at constant 70% and 80% RH and always at 35°C, where this was not possible to be achieved in the laboratory setup. Hence, both laboratory setup and climate chamber complements each other. Additionally, the climate chamber provides better temperature and humidity control, higher results accuracy and allows weighing the desiccant material continuously and automatically in place every minute which was not possible in the laboratory setup that had a disadvantage which is moving the desiccant from the laboratory setup

to be weighed using the balance and then turned back to the laboratory setup, i.e. a manual process.

The profile of the growth of adsorption rate with time is logarithmic, where the curves shown in Figures 6, 8 and 10 are logarithmic curves for all desiccant materials under different conditions of temperature and humidity, except for ARTSorb that showed a linear behavior. On the other side, the mass losses with time through desorption/reactivation process was logarithmic for Silica Gel and Silica Gel Macro-porous, but linear for ARTSorb, PROSorb and the mixture of all desiccants (Figures 13, 15 and 17).

An important notice was that a few beads of desiccant materials, especially Silica Gel, split into two smaller beads after several consecutive sorption and desorption processes. This phenomenon occurs during the sorption process, where they split and spring out of the sieve. Fortunately, this has been noticed during the pilot experiments and not during the main experiments. Therefore, a flat net was placed over the sieve that contains the desiccant material in order to avoid losing weight and giving wrong data. The amount of split beads is approximately 5 g per 100 g of the desiccant material. Unfortunately, this phenomenon will increase the pressure drop through the desiccant segment with time. Therefore, this phenomenon should be further investigated and will lead to determining the lifetime of the desiccant material, i.e. how long it can be packed in the desiccant system and when should it be replaced with new material.

The evaporative cooling pads system usually operates during hot periods which were considered in the calculations equal to 12 h according to Hatem (1993). Table 7 presented the fixed and the variable costs of the desiccant system. However, the operation (variable) costs of the reactivation system should be estimated as well as its fixed costs. Eventually, the costs of both desiccant system and reactivation system should be integrated with the costs of the cooling pads to give a clear overview. Therefore, a lab-scale model and barn

and greenhouse models are highly required to determine the costs as well as the design parameters. The theoretical calculations (Table 7) were performed based on reactivation interval of 150 min and moderate hot humid conditions (25 °C and 50% RH), where the desiccant system theoretically adsorbs 100% of the moisture content in the air and this percentage will decrease with the increasing moisture content and temperature. This implies that the desiccant system will not be designed to adsorb 100% of the moisture and the cooling system and will not reach an efficiency of 100%; rather the desiccant system will adsorb part of the moisture and partially enhance the cooling system efficiency. The number of animals was set based on the statement of Hatem (1993) that typical dairy and poultry barns houses 110 cows and 30,000 birds, respectively. Additionally, Sallvik (1999) stated a number of 570 growing pigs. Furthermore, the size of a small greenhouse was retrieved from the ASABE Standards (2004).

An example on how to interpret the set of data presented in Table 7 can be discussed to implementing the desiccant system for cooling pads in dairy, poultry and pig barns as well as greenhouses. The adsorption capacity -with reactivation every 150 min- is 111 g H₂O per kg of Silica Gel (Table 3). The amount of required desiccant per m² of pads with reactivation is then 70 kg. The thickness of the desiccant segments is 10 cm, having a total pressure drop of 0.6 kPa under the toughest conditions of air velocity of 2.5 m/s and 2 mm bead size. Ultimately, this is requiring 0.18 kW per m² of pads, i.e. 63.5 kWh/m² and month which will cost approximately 12.7 €/(m² month).

Table 8 presents the expected enhancement to the cooling pads efficiency through different conditions of temperature and relative humidity; however, in order to determine the exact values, further experiments are required to be performed in a specially designed lab-scale model of desiccant system and cooling pads and then in barn and greenhouse models. Table 8 shows that the

enhancement percentage is inversely proportional to the water content in the air.

According to the results presented in Tables 2 through 6, Silica Gel has the largest adsorption capacity and the highest adsorption rate with time, fastest change of adsorption rate with time, and the largest moisture content at equilibrium. This is true throughout the different phases of the laboratory setup as well as the climate chamber and under the different conditions, i.e. different temperatures and levels of relative humidity. On the other hand, the performance of Silica Gel Macro-porous is considerably enhanced when reactivated every 150 min or 90 min in comparison to all other desiccant materials. This can be noticed by comparing Tables 2, 3 and 4. The highest performance of ARTSorb was at 70% RH and the lowest was at 90% -100% RH (Tables 2, 5 and 6).

Generally, this study presents a methodology for testing desiccant materials and assessing their suitability for air dehumidification to enhance cooling pads efficiency in animal housing and greenhouses. Therefore, this study recommends using this methodology for testing further desiccant materials for better suitability to the intended application as filling for the desiccant segments that will be mounted next to the cooling pads.

Pereira et al. (2011) stated that the gaseous emissions significantly increase with air temperature. Additionally, the concentrations of the noxious gases inside livestock barns and the gaseous emissions from the barns increase with air temperature (Samer et al., 2011a,b,c, 2012b; Samer and Abuarab, 2014). Accordingly, it can be implied that reducing the indoor air temperature leads to indirectly reduce gaseous emissions (Samer et al., 2011d,e,f). Therefore, it is expected that when implementing the proposed desiccant system to enhance the efficiency of the evaporative cooling pads and consequently improve their ability to reducing the indoor air temperature, the gaseous concentrations inside the livestock barns will be reduced and then the gaseous emissions will be lowered. Hence,

the proposed couple desiccant-pads system will play an important role as a livestock emission abatement technique as discussed by Samer (2013b, 2014, 2015). The design of the barn (Samer, 2010 a, b; Samer 2008b) will affect the ventilation rate and further the airflow profiles (Samer, 2012a,b,c; Samer et al., 2014) and, therefore, this should be investigated in the buildings when the desiccant system is installed.

6 Conclusions

This study shows potential for developing a desiccant system to improving the efficiency of cooling pads for livestock buildings as well as for greenhouses. According to the results of this study, it can be concluded that:

(1). The investigated desiccant materials are suitable for dynamic applications, i.e. adsorbing moisture from air in dynamic motion and in continuous exchange with external air.

(2). The desiccant material must be stable and its solid state must remain unchangeable in order to be suitable as filling material for the desiccant segments.

(3). The adsorption capacity is dependent on the starting conditions (temperature, relative humidity and ventilation rate). According to the results of this study and applied methodology, it was found that one half of the adsorption capacity of the investigated desiccants is attainable after 150 min through the sorption process. Therefore, the desiccant material should be reactivated every 150 min when filled within the desiccant segments of the cooling pads.

(4). The reactivation period is highly dependent on the type of desiccant. This matter must be further investigated in a lab-scale model to minimize the time length of the reactivation to 5-10 minutes which might be achievable through allowing higher volumetric flow rate of hot air driven from the reactivation system.

(5). The profile of the adsorption rate with time through the sorption process is logarithmic for all desiccant materials under different conditions of

temperature and humidity, except for ARTSorb that showed a linear behavior.

(6). The mass loss with time through desorption/reactivation process was logarithmic for Silica Gel and Silica Gel Macro-porous, but linear for ARTSorb, PROSorb and Mixture.

(7). Among all investigated desiccants, Silica Gel has the largest adsorption capacity and the highest adsorption rate, fastest change of adsorption rate, and the largest moisture content at equilibrium.

(8). The proposed couple desiccant-pads system might play an important role as a livestock emission abatement technique.

7 Recommendations for future research

The evaluation of the developed desiccant system should be carried out through the following phases: pilot model, wind tunnel, barn and greenhouse models, and full-scale barn and greenhouse. These procedures can be elaborated as follows: (1) building the pilot model and installing the developed dehumidifying segments on traditional cooling pads then testing the pilot model; (2) testing the aforementioned combination (desiccant system – cooling pads) in wind tunnel to study the effects of wind velocity (speed and direction) on the resulting efficiency of the combined systems; (3) the dehumidifying segments will be further developed and enhanced according to the results of steps (1) and (2); (4) prototyping the desiccant system and testing it in barn and greenhouse models then in full-scale barn and greenhouse in order to study its effects on animals and plants' microclimate. Additional chemicals can be investigated for possible use as desiccant materials for the proposed desiccant system, which are: sodium metal, sodium sulphate anhydrous, calcium sulphate anhydrous, calcium chloride anhydrous, calcium carbide, and charcoal.

References

- Albright, L. D. 1990. *Environment control for animals and plants*. St. Joseph, Michigan, USA: ASAE.
- Al-Helal, I. M. 2007. Effects of ventilation rate on the environment of a fan-pad evaporatively cooled, shaded greenhouse in extreme arid climates. *Transactions of the ASABE*, 23(2): 221-230.
- Armstrong, D. V. 1994. Heat stress interaction with shade and cooling. *Journal of Dairy Science*, 77(7): 2044-2050.
- ASABE Standards. 2008a. Design of ventilation systems for poultry and livestock shelters. Niles Road, St. Joseph, Michigan, USA: ASABE.
- ASABE Standards. 2008b. Heating, ventilating and cooling greenhouses. Niles Road, St. Joseph, Michigan, USA: ASABE.
- ASABE Standards. 2008c. Guidelines for selection of energy efficient agricultural ventilation fans. Niles Road, St. Joseph, Michigan, USA: ASABE.
- ASABE Standards. 2004. Commercial greenhouse design and layout. Niles Road, St. Joseph, Michigan, USA: ASABE.
- Awad, M. M., K. A. Ramy, A. M. Hamed, and M. M. Bekheit. 2008. Theoretical and experimental investigation on the radial flow desiccant dehumidification bed. *Applied Thermal Engineering*, 28(1): 75-85.
- Baehr, H. D., and K. Stephan. 2006. *Heat and mass transfer* (2nd ed.). Berlin, Germany: Springer.
- Bottcher, R. W., L. B. Driggers, T. A. Carter, and A. O. Hobbs. 1992. Field comparison of broiler house mechanical ventilation systems in a warm climate. *Applied Engineering in Agriculture*, 8(4): 499-508.
- Bucklin, R. A., D. R. Bray, J. G. Martin, L. Carlos, and V. Carvalho. 2009. Environmental temperatures in dairy housing. *Applied Engineering in Agriculture*, 25(5): 727-735.
- Bull, R. P., P. C. Harrison, G. L. Riskowski, and H. W. Gonyou. 1997. Preference among cooling systems by gilts under heat stress. *Journal of Animal Science*, 75(8): 2078-2083.
- Chen, C. J., R. Z. Wang, Z. Z. Xia, J. K. Kiplagat, and Z. S. Lu. 2010. Study on a compact silica gel-water adsorption chiller without vacuum valves: Design and experimental study. *Applied Energy*, 87(8): 2673-2681.
- Choi, H.-C., O.-S. Suh, D.-S. Lee, H.-H. Kim, and J.-D. Han. 1998. Comparison of cooling effect by cooling pad and fogging system in windowless laying hen houses. *RDA Journal of Livestock Science*, 40(1): 101-104.
- Collier, R. K. 1989. Desiccant properties and their effect on cooling system performance. *ASHRAE Transactions*, 95, Part 1.
- Dagtekin, M., C. Karaca, and Y. Yildiz. 2009a. Long axis heat distribution in a tunnel-ventilated broiler house equipped with an evaporative pad cooling system. *Animal Production Science*, 49(12): 1125-1131.
- Dagtekin, M., C. Karaca, and Y. Yildiz. 2009b. Performance characteristics of pad evaporative cooling system in a broiler house in a Mediterranean climate. *Biosystems Engineering*, 103(1): 100-104.
- Daragan, V. D., A. Y. Kotov, G. N. Mel'nikov, A. V. Pustogarov, and V. I. Starshinov. 1979. Computation of the pressure loss in gas flow through porous materials. *Inzhenerno-Fizicheskii Zhurnal*, 36(5): 787-794.
- Fiedler, M., K. von Bobrutzki, M. Samer, and W. Berg. 2011. New wind tunnel facility in agricultural research. Proceedings of the International Workshop on Physical Modeling of Flow and Dispersion Phenomena - PHYSMOD2011, August 22-24, Book of Abstracts pp. 118-123, University of Hamburg, Germany.
- Franco, A., D. L. Valera, A. Madueño, and A. Peñá. 2010. Influence of water and air flow on the performance of cellulose evaporative cooling pads used in Mediterranean greenhouses. *Transactions of the ASABE*, 53(2): 565-576.
- Frazzi, E., L. Calamari, and F. Calegari. 2002. Productive response of dairy cows to different barn cooling systems. *Transactions of the ASAE*, 45(2): 395-405.
- Gebremedhin, K. G., P. E. Hillman, C. N. Lee, R. J. Collier, S. T. Willard, J. D. Arthington, and T. M. Brown-Brandl. 2008. Sweating rates of dairy cows and beef heifers in hot conditions. *Transactions of the ASABE*, 51(6): 2167-2178.
- Gebremedhin, K. G., C. N. Lee, P. E. Hillman, and R. J. Collier. 2010. Physiological responses of dairy cows during extended solar exposure. *Transactions of the ASABE*, 53(1): 239-247.
- Grathwohl, P. 1998. *Diffusion in natural porous media: contaminant transport, sorption/desorption and dissolution kinetics*. Norwell, Massachusetts, USA: Kluwer Academic Publishers.
- Gunhan, T., V. Demir, and A. K. Yagcioglu. 2007. Evaluation of the suitability of some local materials as cooling pads. *Biosystems Engineering*, 96(3): 369-377.
- Hall, A. B., B. A. Young, P. J. Goodwing, J. M. Gaughan, and T. Davison. 1997. Alleviation of excessive heat load in the high producing dairy cow. Proceedings of the Fifth International Symposium of Livestock Environment, p. 928-934, ASAE, St. Joseph, Michigan, USA.
- Hatem, M. H. 1993. *Theory of structures and agricultural buildings and environmental control* (2nd ed.). Egypt: Faculty of Agriculture, Cairo University.
- Hatem, M. H., R. R. Sadek, and M. Samer. 2004a. Shed height effect on dairy cows microclimate. *Misr Journal of Agricultural Engineering*, 21(2): 289 - 304.
- Hatem, M. H., R. R. Sadek, and M. Samer. 2004b. Cooling, shed height and shed orientation affecting dairy cows

- microclimate. *Misr Journal of Agricultural Engineering*, 21(3): 714 - 726.
- Hellickson, M. A., and J. N. Walker. 1983. *Ventilation of agricultural structures*. St. Joseph, Michigan, USA: ASAE.
- Huhnke, R. L., L. C. McCowan, G. M. Meraz, S. L. Harp, and M. E. Payto. 2004. Using evaporative cooling to reduce the frequency and duration of elevated temperature-humidity indices. *Transactions of the ASABE*, 20(1): 95–99.
- IPCC. 2007. Climate change 2007: Impacts, adaptation and vulnerability. Contribution of Working Group II to the Fourth Assessment Report of the Intergovernmental Panel on Climate Change [Parry, M.L., O.F. Canziani, J.P. Palutikof, P.J. van der Linden, C.E. Hanson (eds.)]. Cambridge, United Kingdom: Cambridge University Press.
- Johnson, M. F. G., J. M. Zulovich, J. Wurm, R. S. Gates, and L. Turner. 2000. Desiccant system's potential for swine facilities applications. In *Swine Housing, Proc. First Int. Conf. (October 9-11, 2000, Des Moines, Iowa)*, pp. 26-33, St. Joseph, Mich.: ASAE.
- Jiang, M., K. G. Gebremedhin, and L. D. Albright. 2005. Simulation of skin temperature and sensible and latent heat losses through fur layers. *Transactions of the ASABE*, 48(2): 767–775.
- Kittas, C., T. Bartzanas, and A. Jaffrin. 2003. Temperature gradients in a partially shaded large greenhouse equipped with evaporative cooling pads. *Biosystems Engineering*, 85(1): 87-94.
- Kiwan, A., W. Berg, H.-J. Müller, M. Gläser, M. Fiedler, K. von Bobrutski, C. Ammon, M. Samer, and R. Brunsch. 2012. The influence of building equipment and operation on the air exchange rates throughout a naturally ventilated dairy barn. Proceedings of the Ninth International Livestock Environment Symposium (ASABE ILES IX), Paper No. ILES12- 0648, ASABE, July 8-12, Valencia, Spain.
- Koca, R. W., W. C. Hughes, and L. L. Christianson. 1991. Evaporative cooling pads: test procedure and evaluation. *Applied Engineering in Agriculture*, 7(4): 485– 490.
- Liao, C. M., S. Singh, and T. S. Wang. 1998. Characterizing the performance of alternative evaporative cooling pad media in thermal environmental control applications. *Journal of Environmental Science and Health*, 33(7): 1391-1417.
- Lindley, J. A., and J. H. Whitaker. 1996. *Agricultural buildings and structures*. St. Joseph, Michigan, USA: ASAE.
- Liu, Y. L., R. Z. Wang, and Z. Z. Xia. 2005a. Experimental performance of a silica gel–water adsorption chiller. *Applied Thermal Engineering*, 25: 359-375.
- Liu, Y. L., R. Z. Wang, and Z. Z. Xia. 2005b. Experimental study on a continuous adsorption water chiller with novel design. *International Journal of Refrigeration*, 28: 218–230.
- Mekonnen, A., and V. A. Dodd. 1993. Livestock housing in hot arid regions: a study of micro-climate modifiers using a model livestock building. *Agricultural Mechanization in Asia, Africa and Latin America*, 24(3): 27-34.
- Panagakos, P., and P. Axaopoulos. 2006. Simulation comparison of evaporative pads and fogging on air temperatures inside a growing swine building. *Transactions of the ASABE*, 49(1): 209–215.
- Pereira, J., D. Fanguero, T. Misselbrook, D. Chadwick, J. Coutinho, and H. Trindade. 2011. Ammonia and greenhouse gas emissions from slatted and solid floors in dairy cattle houses: a scale model study. *Biosystems Engineering*, 109: 148-57.
- Pesaran, A., and A. Bingham. 1989. Testing of novel desiccant materials and dehumidifier matrices for desiccant cooling applications. Tullie Circle, N.E. Atlanta, GA, USA: ASHRAE.
- Ruthven, D. M. 1984. *Principles of adsorption and adsorption processes*. Hoboken, New Jersey, USA: Wiley-Interscience.
- Sallvik, K. 1999. Environment for animals. In E. Bartali, A. Jongebreur, & D. Moffitt (Eds.), *CIGR Handbook of agricultural Engineering*, Vol. 2 (pp. 31-88). St. Joseph, Michigan, USA: ASAE.
- Samer, M. 2015. GHG Emission from Livestock Manure and its Mitigation Strategies. In: *Climate Change Impact on Livestock: Adaptation and Mitigation*, V. Sejian, J. Gaughan, L. Baumgard & C. Prasad (Eds.), pp. 321-346, ISBN 978-81-322-2264-4, Springer International, Germany.
- Samer, M., and M. E. Abuarab. 2014. Development of CO₂-balance for ventilation rate measurements in naturally cross ventilated dairy barns. *Transactions of the ASABE*, Vol. 57(4): 1255-1264.
- Samer, M., H.-J. Müller, M. Fiedler, W. Berg, and R. Brunsch. 2014. Measurement of ventilation rate in livestock buildings with radioactive tracer gas technique: Theory and methodology. *Indoor and Built Environment*, Vol. 23(5): 692–708.
- Samer, M. 2014. Implementation of nanotechnology and laser radiation to prototype a biological-chemical filter for reducing gas, odor and dust emissions from livestock buildings. Session: Measurement and Mitigation of Pollutants from Livestock and Poultry Housing. Proceedings of the 2014 American Society of Agricultural and Biological Engineers (ASABE) Annual International Meeting, a joint conference with the Canadian Society of Bioengineering (CSBE),

- 13-16.07.2014, Paper No. 141870677, Montreal, Quebec, Canada.
- Samer, M. 2013a. Towards the implementation of the Green Building concept in agricultural buildings: a literature review. *Agricultural Engineering International: CIGR Journal*, Vol. 15(2): 25-46.
- Samer, M. 2013b. Emissions inventory of greenhouse gases and ammonia from livestock housing and manure management. *Agricultural Engineering International: CIGR Journal*, Vol. 15(3): 29–54.
- Samer, M., M. Hatem, H. Grimm, R. Doluschitz, and T. Jungbluth. 2012a. An expert system for planning and designing dairy farms in hot climates. *Agricultural Engineering International: CIGR Journal*, Vol. 14(1): 1-15.
- Samer, M., C. Ammon, C. Loebstin, M. Fiedler, W. Berg, P. Sanftleben, and R. Brunsch. 2012b. Moisture balance and tracer gas technique for ventilation rates measurement and greenhouse gases and ammonia emissions quantification in naturally ventilated buildings. *Building and Environment*, 50(4): 10-20.
- Samer, M., W. Berg, M. Fiedler, K. von Bobrutzki, C. Ammon, P. Sanftleben, and R. Brunsch. 2012c. A comparative study among H₂O-balance, heat balance, CO₂-balance and radioactive tracer gas technique for airflow rates measurement in naturally ventilated dairy barns. Proceedings of the Ninth International Livestock Environment Symposium (ASABE ILES IX), Paper No. ILES12-0079, ASABE, July 8-12, Valencia, Spain.
- Samer, M. 2012a. Effect of airflow profile on reducing heat stress, enhancing air distribution and diluting gaseous concentrations in dairy barns. *Misr Journal of Agricultural Engineering*, Vol. 29(2): 837-856.
- Samer, M. 2012b. A comprehensive study on different methods for air exchange rates measurement in a naturally ventilated dairy house. *Misr Journal of Agricultural Engineering*, Vol. 29(4): 1603-1620.
- Samer, M. 2012c. Reconstruction of old gutter-connected dairy barns: A case study. Proceedings of the 2012 American Society of Agricultural and Biological Engineers (ASABE) Annual International Meeting, 29.07-01.08.2012, Paper No. 121341061, 2012(7), pp. 5401-5418, Dallas, Texas, USA.
- Samer, M., C. Loebstin, M. Fiedler, C. Ammon, W. Berg, P. Sanftleben, and R. Brunsch. 2011a. Heat balance and tracer gas technique for airflow rates measurement and gaseous emissions quantification in naturally ventilated livestock buildings. *Energy and Buildings*, 43(12): 3718-3728.
- Samer, M., M. Fiedler, H.-J. Müller, M. Gläser, C. Ammon, W. Berg, P. Sanftleben, and R. Brunsch. 2011b. Winter measurements of air exchange rates using tracer gas technique and quantification of gaseous emissions from a naturally ventilated dairy barn. *Applied Engineering in Agriculture*, Vol. 27(6): 1015-1025.
- Samer, M., H.-J. Müller, M. Fiedler, C. Ammon, M. Gläser, W. Berg, P. Sanftleben, and R. Brunsch. 2011c. Developing the ⁸⁵Kr tracer gas technique for air exchange rate measurements in naturally ventilated animal buildings. *Biosystems Engineering*, Vol. 109(4): 276-287.
- Samer, M., W. Berg, H.-J. Müller, M. Fiedler, M. Gläser, C. Ammon, P. Sanftleben, and R. Brunsch. 2011d. Radioactive ⁸⁵Kr and CO₂-balance for ventilation rate measurements and gaseous emissions quantification through naturally ventilated barns. *Transactions of the ASABE*, Vol. 54(3): 1137-1148.
- Samer, M., C. Loebstin, K. von Bobrutzki, M. Fiedler, C. Ammon, W. Berg, P. Sanftleben, and R. Brunsch. 2011e. A computer program for monitoring and controlling ultrasonic anemometers for aerodynamic measurements in animal buildings. *Computers and Electronics in Agriculture*, Vol. 79(1): 1-12.
- Samer, M., W. Berg, M. Fiedler, H.-J. Müller, M. Gläser, C. Ammon, R. Brunsch, C. Loebstin, O. Tober, and P. Sanftleben. 2011f. Implementation of radioactive ⁸⁵Kr for ventilation rate measurements in dairy barns. Proceedings of the 2011 American Society of Agricultural and Biological Engineers (ASABE) Annual International Meeting, pp. 847-863, Paper No. 1110679, August 7-10, Louisville, Kentucky, USA.
- Samer, M. 2011a. Effect of cowshed design and cooling strategy on welfare and productivity of dairy cows. *Journal of Agricultural Science and Technology A*, 1(6): 848-857.
- Samer, M. 2011b. Implementation of cooling systems to enhance dairy cows' microenvironment. *Journal of Environmental Science and Engineering*, 5(12): 1654-1661.
- Samer, M. 2010a. Adjusting dairy housing in hot climates to meet animal welfare requirements. *Journal of Experimental Sciences*, 1(3): 14-18.
- Samer, M. 2010b. How to rectify design flaws of dairy housing in hot climates? Proceedings of XVII CIGR World Congress, June 13-17, Book of Abstracts p. 79, Quebec City, Canada.
- Samer, M. 2008. *An expert system for planning and designing dairy farms in hot climates*. PhD dissertation, University of Hohenheim, Stuttgart, Germany. VDI-MEG, ISSN 0931-6264, Script 472.
- Samer, M., H. Grimm, M. Hatem, R. Doluschitz, and T. Jungbluth. 2008a. Spreadsheet modeling to size dairy sprinkler and fan cooling system. Proceedings of Eighth International

- Livestock Environment Symposium (ASABE ILES VIII), pp. 701-708, ASABE, Iguassu Falls City, Brazil.
- Samer, M., H. Grimm, M. Hatem, R. Doluschitz, and T. Jungbluth. 2008b. Mathematical modeling and spark mapping of dairy farmstead layout in hot climates. *Misr Journal of Agricultural Engineering*, Vol. 25(3): 1026 -1040.
- Samer, M. 2004. Engineering parameters affecting dairy cows microclimate and their productivity under Egyptian conditions. M.Sc. Thesis, Cairo University, Egypt.
- Schmidt, G. H., L. D. Van Vleck, and M. F. Hutjens. 1988. *Principles of dairy science*. (2nd ed.). USA: Prentice Hall.
- von Bobrutski, K., M. Samer, A. Kiwan, and W. Berg. 2011. Spreadsheet modeling to compute the air exchange rate in commercial broiler barns. Proceedings of the 5th European Conference on Precision Livestock Farming, July 11-14, Book of Abstracts pp. 326-334, Czech Centre for Science and Society, Prague, Czech Republic.
- Wang, C., W. Cao, B. Li, Z. Shi, and A. Geng. 2008. A fuzzy mathematical method to evaluate the suitability of an evaporative pad cooling system for poultry houses in China. *Biosystems Engineering*, 101(3): 370-375.
- Wang, D.C., J.Y. Wu, Z. Z. Xia, H. Zhai, R. Z. Wang, and W. D. Dou. 2005. Study of a novel silica gel–water adsorption chiller. Part II: Experimental study. *International Journal of Refrigeration*, 28: 1084–1091.
- Wiersma, F., and T. H. Short. 1983. Evaporative cooling. In M. A. Hellickson & J. N. Walker (Eds.), *Ventilation of agricultural structures* (pp. 103-118). St. Joseph, Michigan, USA: ASAE.